Cancer Res 1988;48:793–7; 194. *Anticancer Res* 1995;15:1297–302; 195. *Br J Cancer* 2003;89:185–91; 196. *Tumori* 1989;75:423–8; 197. *Eur J Cancer* 1991;27:673; 198. *Clin Cancer Res* 2003;9:1161–70; 199. *Cancer Res* 2001;61:3986–97; 200. *Mol Cancer Ther* 2002;1:707–17; 201. *Anticancer Res* 2000;20:407–16; 202. *J Biol Chem* 2003;278:23432–40; 203. *Nat Med* 1999;5:662–8; 204. *Oncogene* 2001;20:4995–5004; 205. *Mol Pharmacol* 2002;62:689–97; 206. *Biochem Pharmacol* 2000;59:337–45; 207. *Proc Natl Acad Sci USA* 1991;88:10591–5; 208. *Cancer Res* 1997;57:2721–31; 209. *Mutat Res* 1993;303:113–20; 210. *Anticancer Drugs* 2001;12:829–34; 211. *Di Yi Jun Yi Da Xue Xue Bao* 2002;22:124–6; 212. *Br J Cancer* 1991;63:237–41; 213. *Clin Cancer Res* 1999;5:2588–95; 214. *Cancer* 1994;74:2546–54; 215. *Anticancer Res* 1996;16:1963–70; 216. *Int J Cancer* 1997;73:544–50; 217. *Br J Cancer* 2003;88:624–9; 218. *Oncogene* 2001;20:859–68; 219. *Oncogene* 2000;19:4159–69; 220. *Cancer Sci* 2003;94:467–72; 221. *Cancer Res* 1999;59:811–5; 222. *Nat Med* 1999;5:412–7. 223. *Cancer Res* 1994;54:2287–91; 224. *J Clin Endocrinol Metab* 1998;83:2516–22; 225. *Mol Carcinog* 1995;14:275–85; 226. *Oncogene* 1999;18:477–85; 227. *Cell* 1993;74:957–67; 228. *J Clin Invest* 1999;104:263–9; 229. *Br J Cancer* 1998;77:547–51; 230. *Cancer Res* 1997;57:4285–300; 231. *Breast Cancer Res Treat* 2000;61:211–6; 232. *Anticancer Res* 2000;20:5069–72; 233. *Gynecol Oncol* 2003;90:238–44; 234. *Breast Cancer Res Treat* 1999;58:99–105; 235. *Jpn J Cancer Res* 1998;89:221–7; 236. *Oncogene* 1995;10:2001–6; 237. *Anticancer Res* 2002;22:107–16; 238. *Proc Natl Acad Sci USA* 2003;100:11636–41; 239. *Cancer Cell* 2003;3:403–10; 240. *Cancer Cell* 2003;3:387–402; 241. *Cancer Res* 1994;54:3253–9; 242. *World J Gastroenterol* 1998;4:421–5; 243. *Biochem Cell Biol* 2000;78:119–26; 244. *Mol Cancer Ther* 2004;3:327–34; 245. *Int J Cancer* 1996;67:608–14; 246. *Cancer Res* 1995;55:2576–82; 247. *Gynecol Oncol* 1998;70:398–403; 248. *Chemotherapy* 2002;48:189–95; 249. *Int J Cancer* 2003;106:160–6; 250. *Cancer Res* 2000;60:6052–60; 251. *J Urol* 2001;166:461–9; 252. *J Invest Dermatol* 2003;120:1081–6; 253. *Korean J Intern Med* 1999;14:42–52; 254. *Clin Cancer Res* 2000;6:718–24; 255. *Surg Today* 1997;27:676–9; 256. *Int J Oncol* 2000;16:745–9; 257. *Int J Cancer* 1999;82:860–7; 258. *Eur J Cancer* 2001;37:531–41; 259. *Cancer Chemother Pharmacol* 2002;49:504–10; 260. *Science* 2000;290:989–92; 261. *Cancer Res* 2000;60:7133–41; 262. *Clin Cancer Res* 2003;9:2826–36; 263. *Cancer Sci* 2004;95:44–51; 264. *Cancer Res* 2000;60:2805–9; 265. *Cell Mol Life Sci* 2002;59:1406–12; 266. *Cancer Res* 2000;60:4386–90; 267. *Oncogene* 2002;21:8843–51; 268. *Cancer Res* 2001;61:348–54; 269. *Cancer Res* 1993;53:4443–8; 270. *Breast Cancer Res Treat* 1993;26:23–39; 271. *Eur J Biochem* 1996;237:653–9; 272. *Cancer Res* 1997;57:2661–7; 273. *Breast Cancer Res Treat* 1999;56:187–96.

AZD2171 Shows Potent Antitumor Activity Against Gastric Cancer Over-Expressing Fibroblast Growth Factor Receptor 2/Keratinocyte Growth Factor Receptor

Masayuki Takeda,[1,3] Tokuzo Arao,[1,4] Hideyuki Yokote,[1,4] Teruo Komatsu,[5] Kazuyoshi Yanagihara,[5] Hiroki Sasaki,[6] Yasuhide Yamada,[2] Tomohide Tamura,[2] Kazuya Fukuoka,[7] Hiroshi Kimura,[3] Nagahiro Saijo,[2] and Kazuto Nishio[1,4]

Abstract

Purpose: AZD2171 is an oral, highly potent, and selective vascular endothelial growth factor signaling inhibitor that inhibits all vascular endothelial growth factor receptor tyrosine kinases. The purpose of this study was to investigate the activity of AZD2171 in gastric cancer.

Experimental Design: We examined the antitumor effect of AZD2171 on the eight gastric cancer cell lines *in vitro* and *in vivo*.

Results: AZD2171 directly inhibited the growth of two gastric cancer cell lines (KATO-III and OCUM2M), with an IC_{50} of 0.15 and 0.37 μmol/L, respectively, more potently than the epidermal growth factor receptor tyrosine kinase inhibitor gefitinib. Reverse transcription-PCR experiments and immunoblotting revealed that sensitive cell lines dominantly expressed COOH terminus–truncated fibroblast growth factor receptor 2 (FGFR2) splicing variants that were constitutively phosphorylated and spontaneously dimerized. AZD2171 completely inhibited the phosphorylation of FGFR2 and downstream signaling proteins (FRS2, AKT, and mitogen-activated protein kinase) in sensitive cell lines at a 10-fold lower concentration (0.1 μmol/L) than in the other cell lines. An *in vitro* kinase assay showed that AZD2171 inhibited kinase activity of immunoprecipitated FGFR2 with submicromolar K_i values (~0.05 μmol/L). Finally, we assessed the antitumor activity of AZD2171 in human gastric tumor xenograft models in mice. Oral administration of AZD2171 (1.5 or 6 mg/kg/d) significantly and dose-dependently inhibited tumor growth in mice bearing KATO-III and OCUM2M tumor xenografts.

Conclusions: AZD2171 exerted potent antitumor activity against gastric cancer xenografts overexpressing FGFR2. The results of these preclinical studies indicate that AZD2171 may provide clinical benefit in patients with certain types of gastric cancer.

Various anticancer therapies for gastric cancer have been investigated over the past two decades. Despite intensive studies, the prognosis for patients with unresectable advanced or recurrent gastric cancer remains poor (1, 2), and new therapeutic modalities are needed.

Authors' Affiliations: [1]Shien Lab and [2]Medical Oncology, National Cancer Center Hospital, Tsukiji, Chuo-ku, Tokyo, Japan; [3]Second Department of Internal Medicine, Nara Medical University; [4]Department of Genome Biology, Kinki University School of Medicine, Ohno-higashi, Osaka-Sayama, Osaka, Japan; and [5]Central Animal Lab and [6]Genetic Division, National Cancer Center Research Institute; and [7]Division of Respiratory Medicine, Department of Internal Medicine, Hyogo College of Medicine, Nishinomiya, Hyogo, Japan

Received 11/16/06; revised 1/29/07; accepted 2/27/07.

Grant support: Third-Term Comprehensive 10-Year Strategy for Cancer Control and program for promotion of Fundamental Studies in Health Sciences of the National Institute of Biomedical Innovation and Japan Health Sciences Foundation. The costs of publication of this article were defrayed in part by the payment of page charges. This article must therefore be hereby marked *advertisement* in accordance with 18 U.S.C. Section 1734 solely to indicate this fact.

Note: M. Takeda and T. Arao are the recipient of a Research Resident Fellowship from the Foundation of Promotion of Cancer Research in Japan.

Requests for reprints: Kazuto Nishio, Department of Genome Biology, Kinki University School of Medicine, 377-2 Ohno-higashi, Osaka-Sayama, Osaka 589-8511, Japan. Fax: 81-72-366-0206; E-mail: knishio@med.kindai.ac.jp.

doi:10.1158/1078-0432.CCR-06-2743

Fibroblast growth factors (FGF) and their signaling receptors have been found to be associated with multiple biological activities, including proliferation, differentiation, motility, and transforming activities (3–5). The *K-sam* gene was first identified as an amplified gene in human gastric cancer cell line KATO-III (6, 7), and its product was later found to be identical to the bacteria-expressed kinase, or keratinocyte growth factor receptor (KGFR), and FGF receptor 2 (FGFR2). FGFR2/KGFR/K-sam is preferentially amplified in poorly differentiated types of gastric cancers with a malignant phenotype, and its protein expression was detected by immunohistochemical staining from 20 of 38 cases of the undifferentiated type of advanced stomach cancer (8, 9). Thus, FGFR2 signaling may be as a promising molecular target for gastric cancer.

AZD2171 is a potent, ATP-competitive small molecule that inhibits all vascular endothelial growth factor receptors [VEGFR-1, VEGFR-2 (also known as KDR), and VEGFR-3]. *In vitro* studies have shown that recombinant VEGFR-2 tyrosine kinase activity was potently inhibited by AZD2171 (IC_{50} <1 nmol/L; ref. 10). AZD2171 also showed potent activity versus VEGFR-1 and VEGFR-3 (IC_{50}, 5 and ≤3 nmol/L, respectively). VEGF-stimulated proliferation and VEGFR-2 phosphorylation of human umbilical vascular endothelial cells

was inhibited by AZD2171 (IC_{50}, 0.4 and 0.5 nmol/L, respectively). In *in vivo* studies, inhibition of VEGFR-2 signaling by AZD2171 reduced microvessel density and dose-dependently inhibited the growth of various human tumor xenografts (colon, lung, prostate, breast, and ovary; ref. 10). These data are consistent with potent inhibition of VEGF signaling, angiogenesis, neovascular survival, and tumor growth. On the other hand, because it was known that AZD2171 also possesses additional activity against FGFR1 (IC_{50}, 26 nmol/L; ref. 10), we hypothesized that AZD2171 may exhibit the additional anticancer activity against FGFR-overexpressing gastric cancer cells.

Our previous studies showed significant activities of the dual VEGFR-2 and epidermal growth factor receptor inhibitor ZD6474 against poorly differentiated gastric cancer (11) and non-small-cell lung cancer with epidermal growth factor receptor mutations (12, 13), both *in vitro* and *in vivo*. Based on these findings, we proceeded to investigate the anticancer activity of AZD2171 in preclinical models (gastric cell lines and xenografts).

Materials and Methods

Anticancer agents. AZD2171 and gefitinib (Iressa) were provided by AstraZeneca. AZD2171 and gefitinib were dissolved in DMSO for the *in vitro* experiments, and AZD2171 was suspended in 1% (w/v) aqueous polysorbate 80 and administered in a dose of 0.1 mL/10 g per body weight in the *in vivo* experiments.

Cell culture. Human gastric cancer cell lines 44As3, 58As1, OKAJIMA, OCUM2M, KATO-III, MKN-1, MKN-28, and MKN-74 were maintained in RPMI 1640 (Sigma) supplemented with 10% heat-inactivated fetal bovine serum (Life Technologies) and penicillin-streptomycin.

Established highly tumorigenic cell line. Signet ring cell gastric carcinoma cell line KATO-III was gift from Dr. M. Sekiguchi (University of Tokyo, Tokyo, Japan). All of the presented *in vitro* experiments were done using the KATOIII cell line. We conducted a preliminary experiment to compare the cellular characteristics of TU-KATO-III cells and KATOIII cells, and the results revealed that a high expression level of FGFR2 and high sensitivity to AZD2171 were still maintained in the TU-KATO-III cells (data not shown). KATO-III did not show tumorigenicity following repeated implantation of the cultured cells into BALB/c nude mice. Following s.c. inoculation into nonobese diabetic/severe combined immunodeficient mice, 80% to 100% of the KATO-III cells caused the formation of tumor. Following this result, we cultured the cancer cells isolated from the tumor of mice that developed 2 to 3 months following the implantation of KATO-III cells and attempted s.c. injection into nude mice, in turn, of the incubated cells. This sequence of manipulations was repeated for seven cycles in an attempt to reliably isolate cell lines that would have higher potential to undergo tumor formation over short periods of time. In this way, we obtained a cell line (TU-kato-III) from KATO-III cells that possessed a high tumorigenic potential.

In vitro *growth inhibition assay.* The 3-(4,5-dimethylthiazol-2-yl)-2,5-diphenyltetrazolium bromide assay was used to evaluate the growth-inhibitory effect of AZD2171. Cell suspensions (180 μL) were seeded into each well of 96-well microculture plate and incubated in 10% fetal bovine serum medium for 24 h. The cells were exposed to AZD2171 or gefitinib at concentrations ranging from 4 nmol/L to 80 μmol/L and cultured at 37°C in a humidified atmosphere for 72 h. After the culture period, 20 μL 3-(4,5-dimethylthiazol-2-yl)-2,5-diphenyltetrazolium bromide reagent was added, and the plates were incubated for 4 h. After centrifugation, the culture medium was discarded, and wells were filled with DMSO. The absorbance of the cultures at 562 nmol/L was measured using Delta-soft on a Macintosh computer (Apple) interfaced to a Bio-Tek Microplate Reader EL-340 (BioMatellics). This experiment was done in triplicate.

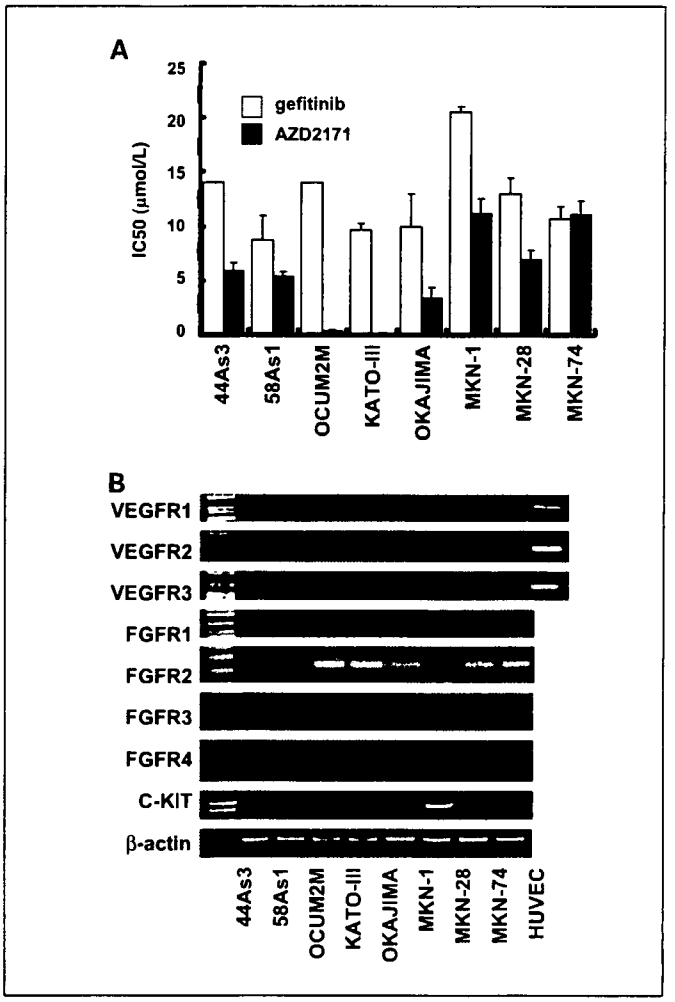

Fig. 1. *A, in vitro* growth-inhibitory effect of AZD2171 and gefitinib on eight gastric cancer cell lines. AZD2171 had a growth-inhibitory effect on KATO-III cells and OCUM2M cells (IC_{50}, 0.15 and 0.37 μmol/L, respectively). Columns, mean IC_{50} of each compound from three independent experiments; bars, SD. □, IC_{50} of gefitinib; ■, IC_{50} of AZD2171. *B,* the mRNA expression levels of VEGFRs, FGFRs, and c-KIT in gastric cancer cell lines were determined by reverse transcription-PCR. Human umbilical vascular endothelial cells were used as the positive control for the VEGFRs. No mRNA expression of VEGFRs or c-KIT was detected by reverse transcription-PCR in both sensitive cell lines, but FGFR2 was strongly detected; however, little faint or none was detected in the other cell lines.

Reverse-transcription PCR. Using a GeneAmp RNA-PCR kit (Applied Biosystems), 5 μg of total RNA from each cultured cell line was converted to cDNA. The PCR amplification procedure consisted of 28 to 35 cycles (95°C for 45 s, 62°C for 45 s, and 72°C for 60 s) followed by incubation at 72°C for 7 min, and the bands were visualized by ethidium bromide staining. The following primers were used for the PCR: human-specific β-actin, forward 5-GGAAATCGTGCGTGACATT-3 and reverse 5-CATCTGCTGGAAGGTGGACAG-3; VEGFR-1, forward 5-TAGCGTCACCAGCAGCGAAAGC-3 and reverse 5-CCTTTCTTTTGGGTCTCTGTGC-3; VEGFR-2, forward 5-CAGACGGACAGTGGTATGGTTC-3 and reverse 5-ACCTGCTGGTGGAAAGAACAAC-3; VEGFR-3, forward 5-AGCCATTCATCAACAAGCCT-3 and reverse 5-GGCAACAGCTGGATGTCATA-3; c-KIT, forward 5-GCCCACAATAGATTGGTATTT-3 and reverse 5-AGCATCTTTACAGCGACAGTC-3; FGFR1, forward 5-GGAGGATCGAGCTCACTCGTGG-3 and reverse

5-CGGAGAAGTAGGTGGTGTCAC-3; FGFR2, forward 5-CAGTAGGACTGTAGACAGTGAA-3 and reverse 5-CCGGTGAGGCGATCGCTCCACA-3; FGFR3, forward 5-GGTCAAGGATGGCACAGGGCTG-3 and reverse 5-AGCAGCTTCTTGTCCATCCGCT-3; and FGFR4, forward 5-CCGCCTAGAGATTGCCAGCTTC-3 and reverse 5-AGGCCTGTCCATCCTTAAGCCA-3.

Real-time reverse transcription-PCR. Real-time reverse transcription-PCR amplification was done by using a Premix Ex Taq and Smart Cycler system (Takara Bio, Inc.) according to the manufacturer's instructions. The following primers were used: FGFR2 (IIIb), forward 5-GATAAATAGTTCCAATGCAGAAGTGCT-3 and reverse 5-TGCCCTATATAATTGGAGACCTTACA-3 (7); FGFR2 (COOH-terminal), forward 5-GAATACTTGGACCTCAGCCAA-3 and reverse 5-AACACTGCCGTTTATGTGTGG-3; and human-specific β-actin, forward 5-GGAAATCGTGCGTGACATT-3 and reverse 5-CATCTGCTGGAAGGTGGACAG-3. The experiment was independently done in triplicate using β-actin as a reference to normalize the data.

Western blotting. Cells were cultured overnight in 10% serum-containing medium or serum-starved medium and exposed to 0.1 to 10 μmol/L of AZD2171 for 3 h before addition of KGF (100 ng/mL) for 15 min. Immunoblotting was done as described previously (14). In brief, after lysing the cells in radioimmunoprecipitation buffer, the lysate was electrophoresed through 10% (w/v) polyacrylamide gels. The proteins were transferred to polyvinylidene difluoride membranes and reacted with the following antibodies: anti-FGFR2 (H-80) and anti-FGFR2 (C-17) antibody (Santa Cruz Biotechnology, Inc.); anti-phosphotyrosine antibody PY20 (BD Transduction Laboratories); anti-phosphorylated FGFR (Tyr653/654), anti-mitogen-activated protein kinase, anti-phosphorylated mitogen-activated protein kinase antibody, anti-AKT, anti-phosphorylated AKT, and anti-rabbit horseradish peroxidase-conjugated antibody (Cell Signaling Technology); and anti-β-actin antibody (Sigma). Visualization was achieved with an enhanced chemiluminescent detection reagent (Amersham Bioscience).

FGFR2 kinase assay. FGFR2/KGFR kinase activity was quantified by using a Universal Tyrosine Kinase Assay kit (Takara) according to manufacturer's instructions. FGFR2/KGFR proteins were collected from the KATO-III, OCUM2M, and OKAJIMA cell lysates by overnight immunoprecipitation with an anti-FGFR2 antibody. The FGFR2/KGFR immune complexes were washed thrice with radioimmunoprecipitation assay buffer and diluted kinase reaction buffer. Immobilized tyrosine kinase substrate (poly[Glu-Tyr]) was incubated for 30 min at 37°C with each sample in the presence of kinase-reacting solution and ATP. Samples were washed four times, blocked with blocking solution, and incubated with anti-phosphotyrosine antibody (PY20) conjugated to horseradish peroxidase. The absorbance of the phosphorylated substrate was measured at 450 nm.

Chemical cross-link analysis. The chemical cross-link analysis was carried out as described previously (15). In brief, KATO-III cells and OKAJIMA cells were cultured under serum-starved conditions for 24 h, and after stimulation with KGF (100 ng/mL) for 15 min, they were collected and washed with PBS and incubated for 30 min in PBS

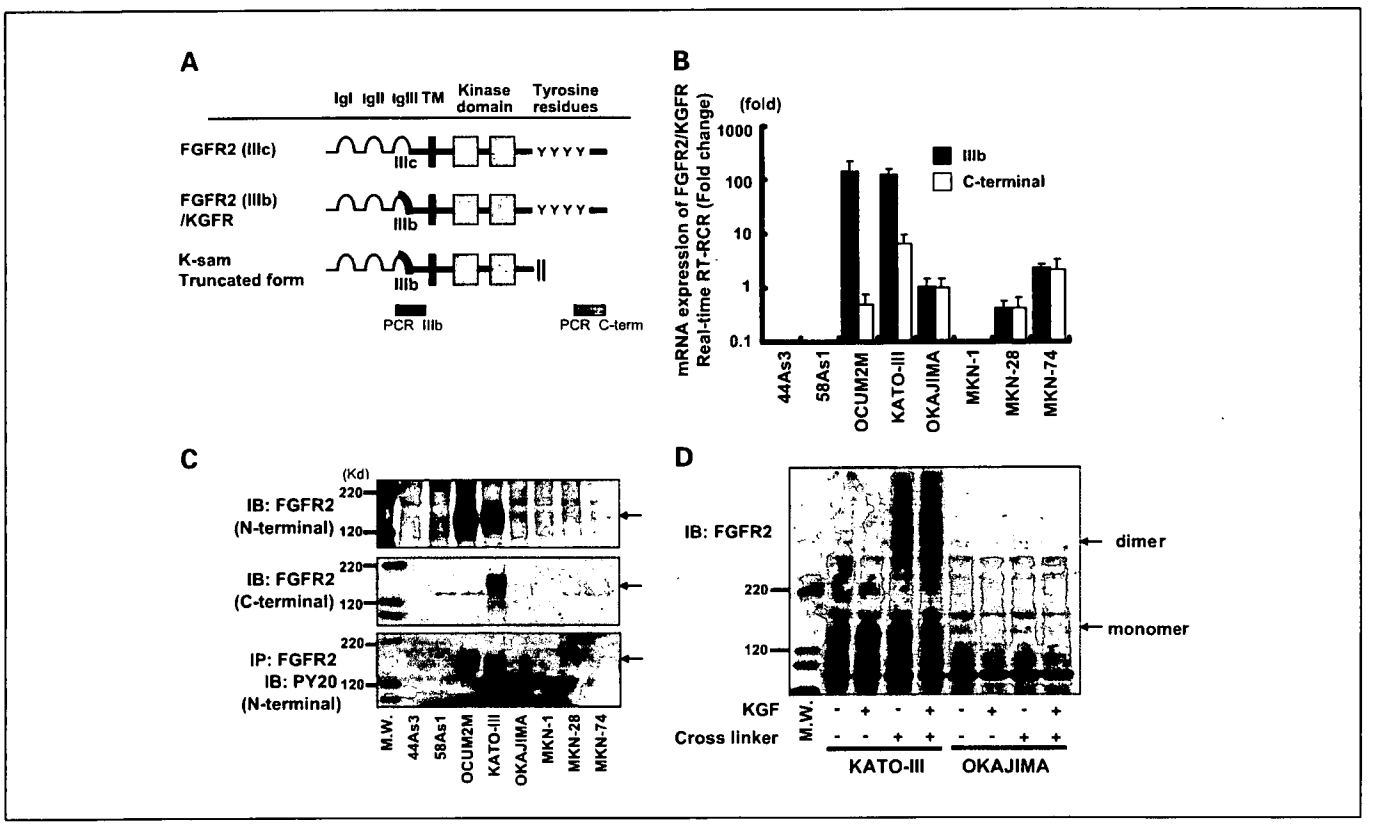

Fig. 2. *A*, schematic representation of FGFR2 and regions amplified by PCR. *B*, mRNA expression levels of FGFR2 were quantified by detecting the extracellular domain or COOH-terminal region by real-time reverse transcription-PCR. Expression in the cells is shown as a ratio to expression in OKAJIMA cells. FGFR2 was overexpressed in KATO-III cells and OCUM2M cells by about 100-fold compared with the other cell lines. The majority of the FGFR2 in the sensitive cell lines KATO-III and OCUM2M had no COOH-terminal region. *C*, protein expression levels of FGFR2 were determined by Western blotting with antibodies to the NH_2 or COOH termini. Both AZD2171-sensitive cell lines overexpressed FGFR2, and the phosphorylation levels were markedly higher. *D*, chemical cross-linking analysis. Cells were cultured under serum-starved conditions for 24 h and then stimulated with KGF (100 ng/mL) for 15 min. After collecting and washing them with PBS, they were incubated for 30 min in PBS containing cross-linker substrate. The reaction was terminated by adding 250 mmol/L glycine for 5 min. In spite of the serum-starved conditions, high levels of expression of the dimerized form were observed in KATO-III cells in the absence of ligand stimulation. This phenomenon was not observed in the control undifferentiated OKAJIMA cell line. Ligand stimulation resulted in a mild increase in the dimerized form in KATO-III cells. Arrows indicate monomer or dimer formation.

containing 1.5 mmol/L of the non-permeable cross-linker bis-(sulfosuccinimidyl) substrate (Pierce). The reaction was terminated by adding 250 mmol/L glycine for 5 min, and the cells were analyzed by immunoblotting with FGFR2 antibody (Sigma).

FGFR2/KGFR gene silencing with small interfering RNA. Predesigned small interfering RNA (siRNA) targeting FGFR2 was purchased from Ambion. KATO-III cells were plated on a 96-well plate and incubated in serum-containing medium for 24 h. The cells were then transfected with the FGFR2 targeting siRNA or non-silencing siRNA using RNAiFect Transfection Reagent (Qiagen) according to the manufacturer's protocol and incubated another 72 h. Cell growth was evaluated by the 3-(4,5-dimethylthiazol-2-yl)-2,5-diphenyltetrazolium bromide assay. For immunoblotting, 2×10^5 cells per well were plated on a six-well plate for 24 h and transfected with siRNA under the same conditions.

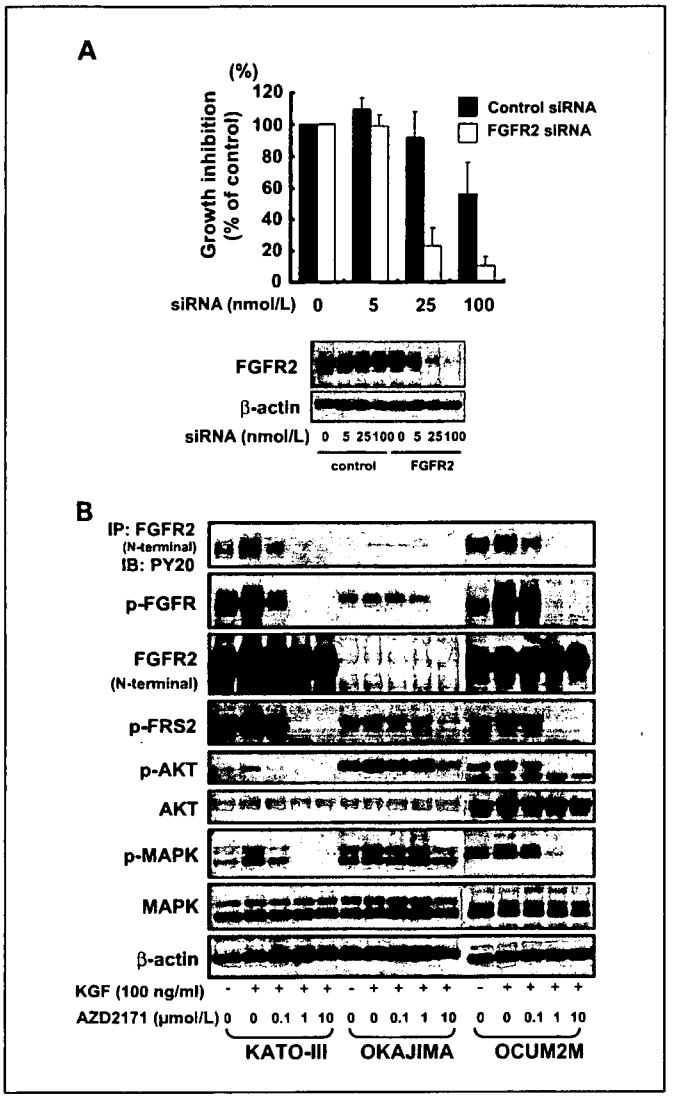

Fig. 3. *A*, FGFR2 targeting siRNA and cellular growth-inhibitory effect. KATO-III cells were plated on a 96-well plate and incubated in serum-containing medium for 24 h. After incubation, the cells were transfected with FGFR2-targeting or non-silencing siRNA and incubated for another 72 h. Cell growth was evaluated by 3-(4,5-dimethylthiazol-2-yl)-2,5-diphenyltetrazolium bromide assay. For immunoblotting, 2×10^5 cells per well were plated on a six-well plate and treated similarly. Marked inhibition of cell growth (~80%) was observed by FGFR2 targeting siRNA compared with control siRNA (*top*). Reduction of FGFR2 protein expression in KATO-III cells was confirmed by immunoblotting (*bottom*). Columns, % control absorbance in three independent experiments; bars, SD. *B*, Western blotting for downstream molecules of FGFR2 signaling. Cells were cultured overnight under serum-starved conditions and exposed to 0.1 to 10 μmol/L AZD2171 for 3 h before adding 100 ng/mL KGF for 15 min. AZD2171 completely inhibited KGF-induced phosphorylation of FGFR2 at 1 μmol/L in the sensitive cell lines, compared with 10 μmol/L in the control cell line OKAJIMA. Similar results were observed for FRS-2, AKT, and mitogen-activated protein kinase (*MAPK*).

In vivo *experiments.* Tumorigenic TU-kato-III cells were derived from the gastric cancer cell line KATO-III. Four-week-old female BALB/c nude mice were purchased from CLEA Japan, Inc. and maintained under specific-pathogen-free conditions; 5×10^6 TU-kato-III cells or OCUM2M cells were s.c. injected into both flanks of each mouse. When the tumors had reached a volume of 0.1-0.3 cm^3, the mice were randomized into three groups (three per group) and given AZD2171, 1.5 or 6.0 mg/kg/d, or vehicle once daily by oral gavage for 3 weeks. Tumor volume was calculated using the formula: (length × width) × $\sqrt{}$(length × width) × (π/6), where length is the longest diameter across the tumor, and width is the corresponding perpendicular. All mice were sacrificed on day 21, and the tumors were collected. The protocol of the experiment was approved by the Committee for Ethics in Animal Experimentation and conducted in accordance with the Guidelines for Animal Experiments of National Cancer Center.

Results

AZD2171 showed growth-inhibitory activity **in vitro.** To evaluate the growth-inhibitory activity of AZD2171 *in vitro*, we did 3-(4,5-dimethylthiazol-2-yl)-2,5-diphenyltetrazolium bromide assays on eight gastric cancer cell lines. The epidermal growth factor receptor–specific tyrosine kinase inhibitor gefitinib was used as a reference. The IC_{50} of gefitinib for all cell lines was between 7 and 20 μmol/L. AZD2171 inhibited the growth of KATO-III cells and OCUM2M cells (IC_{50}, 0.15 and 0.37 μmol/L, respectively) more potently than the other cell lines (Fig. 1A).

Expression levels of tyrosine kinase receptors. To elucidate the mechanism of action of AZD2171 in the two sensitive cell lines, we measured mRNA expression levels of VEGFRs, FGFRs, and c-KIT, whose kinase activity have been reported to be inhibited by AZD2171 (10). No mRNA expression of VEGFRs or c-KIT was detected by reverse transcription-PCR in either sensitive cell lines. FGFR2 transcripts, however, were strongly expressed in both sensitive cell lines but not strongly in the other cell lines (Fig. 1B). Since we previously found that FGFR2/KGFR/K-sam with a deletion of COOH-terminal exons was amplified in both sensitive cell lines (9), we speculated that amplified FGFR2/KGFR might be associated with sensitivity to AZD2171.

Sensitive cells expressed constitutively active and spontaneously dimerized FGFR2/KGFR. We quantified mRNA expression levels of FGFR2 by real-time reverse transcription-PCR with primers that detect the extracellular domain (IIIb region, see Fig. 2A) and COOH-terminal region. The results show that KATO-III cells and OCUM2M cells expressed FGFR2 100-fold higher than the other cells tested. The COOH-terminal region of FGFR2 was deleted in the KATO-III cells and OCUM2M cells (Fig. 2B). Overexpression and markedly increased phosphorylation of FGFR2 was observed in the AZD2171-sensitive cell lines (Fig. 2C).

Immunoblotting with antibodies for the COOH and NH_2 termini revealed that almost all the FGFR2 expressed by OCUM2M cells, and about half of FGFR2 expressed by KATO-III cells, were truncated (Fig. 2C). Although the KATO-III cells expressed wild-type receptor to some extent, the

Table 1. *In vitro* kinase assay of AZD2171 against FGFR2

Cell line	K_m	K_i (μmol/L)
KATO-III	8.3 ± 3.3	0.067 ± 0.017
OCUM2M	7.1 ± 1.4	0.072 ± 0.022
OKAJIMA	11.0 ± 5.0	0.049 ± 0.041

COOH-terminal truncated type was dominantly expressed in AZD2171-sensitive cell lines.

A chemical cross-linking analysis was done to evaluate the dimerization of FGFR2. High dimerization of FGFR2 was observed in the KATO-III cells even in the absence of ligand stimulation (Fig. 2D), but no such phenomenon was observed in the control undifferentiated OKAJIMA cell line. Ligand stimulation increased the level of the dimerized-form in KATO-III cells. Taken together, these findings show that the sensitive cell lines expressed high levels of FGFR2 that was highly phosphorylated and spontaneously dimerized without ligand stimulation, suggesting that FGFR2 signaling is constitutively activated in these cells. This evidence is consistent with the widely recognized findings that cancer cells sensitive to other tyrosine kinase inhibitors, such as gefitinib and imatinib, overexpress the highly phosphorylated target receptor with an increased level of dimerization in a ligand-independent manner (12, 16, 17).

FGFR2 targeting siRNA showed a potent growth-inhibitory effect on KATO-III cells. To investigate the dependency of cell growth through activated FGFR2 signaling in the AZD2171-sensitive KATO-III cell line, we evaluated the growth-inhibitory effect of siRNA targeted to FGFR2 in KATO-III cells. Targeted siRNA (5-100 nmol/L) decreased FGFR2 and inhibited cell growth (>80%) in a dose-dependent manner (Fig. 3A). The results show that most of the growth of KATO-III cells is dependent on activated FGFR2 signaling, suggesting that the FGFR signaling dependency may be responsible for the higher growth-inhibitory effect of AZD2171 on KATO-III cells.

AZD2171 inhibited FGFR2 signaling. Next, we examined the effect of AZD2171 on FGFR2 downstream phosphorylation signals (i.e., FRS-2, AKT, and mitogen-activated protein kinase). AZD2171 completely inhibited KGF-induced phosphorylation of FGFR2, FRS-2, AKT, and mitogen-activated protein kinase at 1 μmol/L in KATO-III cells, compared with 10 μmol/L in OKAJIMA cells. These results clearly show that AZD2171 possesses inhibitory activity against FGFR2 in cell-based studies and significantly inhibits the phosphorylation of FGFR2 at 1 μmol/L in sensitive cells.

FGFR2 kinase inhibition of AZD2171. To quantify the inhibitory activity of AZD2171 on FGFR2 kinase under cell-free conditions, we calculated the K_i values for immunoprecipitated FGFR2 derived from KATO-III, OCUM2M, and OKAJIMA cells. The K_i values of AZD2171 for FGFR2 in each of these cell lines were 0.067 ± 0.017, 0.072 ± 0.022, and 0.049 ± 0.041 μmol/L, respectively (Table 1). In contrast, the K_i value of AZD2171 for recombinant VEGFR-2 was 0.0009 μmol/L (data not shown) and was consistent with previous reports (10). At the cellular level, phosphorylation of

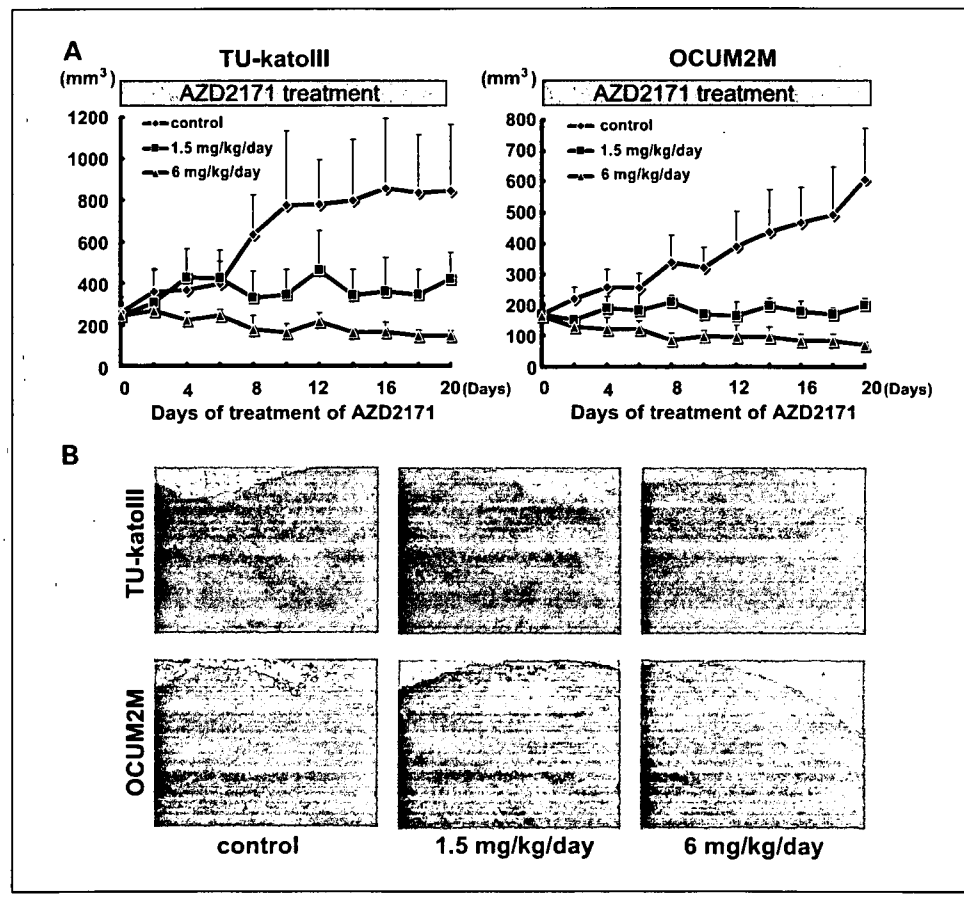

Fig. 4. *A, in vivo* growth-inhibitory effect of AZD2171 in a tumor xenograft model. After s.c. injecting 5 × 10^6 TU-kato-III or OCUM2M cells into both flanks of the mice, AZD2171 (1.5 or 6.0 mg/kg/d), or vehicle, was administered orally once daily for 3 wks. A marked tumor growth-inhibitory effect was observed at the low dose (1.5 mg/kg/d) of AZD2171 in both the TU-kato-III tumors and OCUM2M tumors, and the high dose (6.0 mg/kg/d) of AZD2171 completely inhibited the growth of both cell lines. *B*, representative H&E staining of tumor tissue from mice treated with AZD2171. Broad dose-dependent necrosis was observed. Original magnification, ×40.

FGFR2 was inhibited at 10-fold lower concentrations of AZD2171 in the sensitive cell lines (Fig. 3B), but there were no marked differences between the kinase-inhibitory effects among the proteins derived from the cell lines in this cell-free assay. This discrepancy is discussed in the Discussion.

In vivo *antitumor activity of AZD2171 against FGFR2-overexpressing gastric cancer.* To elucidate the *in vivo* antitumor activity of AZD2171 in mice bearing gastric cancer tumor xenografts, we used the newly established tumorigenic subline TU-kato-III (derived from KATO-III) and OCCUM2M. We attempted to perform control experiments using OKAJIMA cells *in vivo* as suggested by the reviewer. Unfortunately, however, the cell lines grew slowly in the mice, and we could not precisely evaluate the antitumor activity of AZD2171 in the model. However, the results of preliminarily experiments showed that AZD2171 seemed to be less effective against OKAJIMA cells than against KatoIII and OCUM2M cell *in vivo*. Mice implanted the TU-kato-III and OCUM2M tumors were given a low or high dose of AZD2171 (i.e., 1.5 or 6.0 mg/kg/d), or vehicle, orally for 3 weeks. AZD2171 (1.5 mg/kg/d) significantly inhibited tumor growth in the mice bearing TU-kato-III and OCUM2M tumors, and the higher dose (6.0 mg/kg/d) completely inhibited the growth of both tumor models (Fig. 4A). H&E staining showed broad dose-dependent necrosis of core tumor tissue in mice treated with AZD2171 (Fig. 4B). Thus, AZD2171 showed marked antitumor activity *in vivo* against both human gastric tumor xenografts.

Discussion

Recent studies have shown that FGFRs and their ligands are promising therapeutic target molecules for various malignant diseases, such as prostate cancer (18), breast cancer (5, 19), endometrial carcinoma (20), synovial sarcomas (21), thyroid carcinoma (22, 23), and hematopoietic malignancies (24–27). These findings are based on the biological properties of malignant cells expressing activated FGFR, like FGFR fusion tyrosine kinase, involved in chromosomal translocations, gene amplification of FGFRs, or overexpression of FGFs (5, 18–27). In the case of gastric cancer, the results of immunohistochemical analysis of clinical samples revealed that 20 of 38 cases of advanced undifferentiated type of gastric cancer were FGFR2/K-sam positive, whereas none of the 11 cases with the differentiated or intestinal type of cancer showed positive staining for K-sam (8). The results suggest that FGFR2/K-sam overexpression is associated with the undifferentiated type of stomach cancers. The results of fluorescence *in situ* hybridization analysis of the gastric cancer specimens showed gene amplification of FGFR2/K-sam in 2.9% (28). The clinical implication of FGFR2 overexpression/amplification in gastric cancers remains to be fully clarified, and further investigation is needed.

AZD2171 has the most potent kinase-inhibitory activity against VEGFR-2 (IC_{50} < 1 nmol/L); it also possesses additional activity against VEGFR-1, VEGFR-3, and c-Kit (IC_{50}, 5, ≤3, and 2 nmol/L, respectively; ref. 10). AZD2171 showed antiangiogenic activity and broad antitumor activity consistent with potent inhibition of VEGF-induced angiogenesis. We showed kinase-inhibitory activity of AZD2171 against FGFR2 in the present study. When cancer cells are dependent on FGFR2 signaling, AZD2171 can be expected to give additional therapeutic benefit in addition to its antiangiogenic effects.

A cell-based Western blotting analysis showed that phosphorylation of FGFR2 in KATO-III cells and OCUM2M cells was inhibited by AZD2171 at 10-fold lower dose than in OKAJIMA cells (Fig. 3B). However, there was no significant difference in the K_i values of AZD2171 between the FGFR2 derived from KATO-III, OCUM2M, and OKAJIMA in an *in vitro* kinase assay. This may be attributable to the different conditions between the cell-based and cell-free assays. For example, undefined intrinsic intracellular factors may influence kinase activity: (*a*) differences in baseline intracellular FGFR2 phosphatase activity in each cell line, (*b*) differences in intracellular concentration of ([transporters, such as ATP-binding cassette transporters, may be involved in this phenomenon refs. 29, 30), and (*c*) undefined intrinsic inhibitory factors that bind the compounds directly may also be involved (e.g., Brehmer D, et al. have identified various gefitinib binding proteins by affinity chromatography; ref. 31).

In conclusion, AZD2171, a potent inhibitor of all VEGFRs (VEGFR-1, VEGFR-2, and VEGFR-3), was found to have antitumor effect against gastric cancer xenografts in line with previous findings in colon, lung, prostate, breast, and ovarian tumor xenografts (10). The results of this study suggest that activation of the FGFR2 pathway may be a promising target for gastric cancer therapy. AZD2171 may provide a clinical benefit to gastric cancer patients.

Acknowledgments

We thank Dr. T. Komatsu and M. Takigahira for the animal study and Dr. K. Hirakawa (Osaka City University Graduate School of Medicine, Osaka, Japan) for providing the OCUM2M cell line.

References

1. Vanhoefer U, Rougier P, Wilke H, et al. Final results of a randomized phase III trial of sequential high-dose methotrexate, fluorouracil, and doxorubicin versus etoposide, leucovorin, and fluorouracil versus infusional fluorouracil and cisplatin in advanced gastric cancer: a trial of the European Organization for Research and Treatment of Cancer Gastrointestinal Tract Cancer Cooperative Group. J Clin Oncol 2000;18:2/648–57.
2. Ohtsu A, Shimada Y, Shirao K, et al. Randomized phase III trial of fluorouracil alone versus fluorouracil plus cisplatin versus uracil and tegafur plus mitomycin in patients with unresectable, advanced gastric cancer: The Japan Clinical Oncology Group Study (JCOG9205). J Clin Oncol 2003;21:54–9.
3. Grose R, Dickson C. Fibroblast growth factor signaling in tumorigenesis. Cytokine Growth Factor Rev 2005;16:179–86.
4. Itoh H, Hattori Y, Sakamoto H, et al. Preferential alternative splicing in cancer generates a K-sam messenger RNA with higher transforming activity. Cancer Res 1994;54:3237–41.
5. Moffa AB, Tannheimer SL, Ethier SP. Transforming potential of alternatively spliced variants of fibroblast growth factor receptor 2 in human mammary epithelial cells. Mol Cancer Res 2004;2:643–52.
6. Nakatani H, Sakamoto H, Yoshida T, et al. Isolation of an amplified DNA sequence in stomach cancer. Jpn J Cancer Res 1990;81:707–10.
7. Hattori Y, Odagiri H, Nakatani H, et al. K-sam, an amplified gene in stomach cancer, is a member of the heparin-binding growth factor receptor genes. Proc Natl Acad Sci U S A 1990;87:5983–7.
8. Hattori Y, Itoh H, Uchino S, et al. Immunohistochemical detection of K-sam protein in stomach cancer. Clin Cancer Res 1996;2:1373–81.
9. Ueda T, Sasaki H, Kuwahara Y, et al. Deletion of the carboxyl-terminal exons of K-sam/FGFR2 by short homology-mediated recombination, generating preferential expression of specific messenger RNAs. Cancer Res 1999;59:6080–6.
10. Wedge SR, Kendrew J, Hennequin LF, et al. AZD2171: a highly potent, orally bioavailable, vascular

endothelial growth factor receptor-2 tyrosine kinase inhibitor for the treatment of cancer. Cancer Res 2005;65:4389–400.

11. Arao T, Yanagihara K, Takigahira M, et al. ZD6474 inhibits tumor growth and intraperitoneal dissemination in a highly metastatic orthotopic gastric cancer model. Int J Cancer 2006;118:483–9.
12. Arao T, Fukumoto H, Takeda M, et al. Small in-frame deletion in the epidermal growth factor receptor as a target for ZD6474. Cancer Res 2004;64:9101–4.
13. Taguchi F, Koh Y, Koizumi F, et al. Anticancer effects of ZD6474, a VEGF receptor tyrosine kinase inhibitor, in gefitinib ("Iressa")-sensitive and resistant xenograft models. Cancer Sci 2004;95:984–9.
14. Koizumi F, Kanzawa F, Ueda Y, et al. Synergistic interaction between the EGFR tyrosine kinase inhibitor gefitinib ("Iressa") and the DNA topoisomerase I inhibitor CPT-11 (irinotecan) in human colorectal cancer cells. Int J Cancer 2004;108:464–72.
15. Koizumi F, Shimoyama T, Taguchi F, Saijo N, Nishio K. Establishment of a human non-small cell lung cancer cell line resistant to gefitinib. Int J Cancer 2005; 116:36–44.
16. Sakai K, Arao T, Shimoyama T, et al. Dimerization and the signal transduction pathway of a small in-frame deletion in the epidermal growth factor receptor. FASEB J 2006;20:311–3.17. Duensing A, Heinrich MC, Fletcher CD, Fletcher JA. Biology of gastrointestinal stromal tumors: KIT mutations and beyond. Cancer Invest 2004;22:106–16.
18. Gowardhan B, Douglas DA, Mathers ME, et al. Evaluation of the fibroblast growth factor system as a potential target for therapy in human prostate cancer. Br J Cancer 2005;92:320–7.
19. Zang XP, Nguyen TN, Pento JT. Specific and non-specific KGF inhibition of KGF-induced breast cancer cell motility. Anticancer Res 2002;22:2539–45.
20. Taniguchi F, Harada T, Sakamoto Y, et al. Activation of mitogen-activated protein kinase pathway by keratinocyte growth factor or fibroblast growth factor-10 promotes cell proliferation in human endometrial carcinoma cells. J Clin Endocrinol Metab 2003;88: 773–80.
21. Ishibe T, Nakayama T, Okamoto T, et al. Disruption of fibroblast growth factor signal pathway inhibits the growth of synovial sarcomas: potential application of signal inhibitors to molecular target therapy. Clin Cancer Res 2005;11:2702–12.
22. St Bernard R, Zheng L, Liu W, et al. Fibroblast growth factor receptors as molecular targets in thyroid carcinoma. Endocrinology 2005;146:1145–53.
23. Ezzat S, Huang P, Dackiw A, Asa SL. Clin Dual inhibition of RET and FGFR4 restrains medullary thyroid cancer cell growth. Cancer Res 2005;11:1336–41.
24. Chen J, Lee BH, Williams IR, et al. FGFR3 as a therapeutic target of the small molecule inhibitor PKC412 in hematopoietic malignancies. Oncogene 2005;24: 8259–67.
25. Trudel S, Li ZH, Wei E, et al. CHIR-258, a novel, multitargeted tyrosine kinase inhibitor for the potential treatment of t(4;14) multiple myeloma. Blood 2005; 105:2941–8.
26. Delaval B, Letard S, Lelievre H, et al. Oncogenic tyrosine kinase of malignant hemopathy targets the centrosome. Cancer Res 2005;65:7231–40.
27. Chen J, Deangelo DJ, Kutok JL, et al. PKC412 inhibits the zinc finger 198-fibroblast growth factor receptor 1 fusion tyrosine kinase and is active in treatment of stem cell myeloproliferative disorder. Proc Natl Acad Sci U S A 2004;101:14479–84.
28. Hara T, Ooi A, Kobayashi M, Mai M, Yanagihara K, Nakanishi I. Amplification of c-myc, K-sam, and c-met in gastric cancers: detection by fluorescence *in situ* hybridization. Lab Invest 1998;9:43–53.
29. Yanase K, Tsukahara S, Asada S, Ishikawa E, Imai Y, Sugimoto Y. Gefitinib reverses breast cancer resistance protein-mediated drug resistance. Mol Cancer Ther 2004;3:1119–25.
30. Elkind NB, Szentpetery Z, Apati A, et al. Multidrug transporter ABCG2 prevents tumor cell death induced by the epidermal growth factor receptor inhibitor Iressa (ZD1839, Gefitinib). Cancer Res 2005;65:1770–7.
31. Brehmer D, Greff Z, Godl K, et al. Cellular targets of gefitinib. Cancer Res 2005;65:379–82.

CHEST

Original Research

LUNG CANCER

Detection of Epidermal Growth Factor Receptor Mutation in Transbronchial Needle Aspirates of Non-Small Cell Lung Cancer*

Atsushi Horiike, MD; Hideharu Kimura, MD, PhD; Kazuto Nishio, MD, PhD; Fumiyoshi Ohyanagi, MD, PhD; Yukitoshi Satoh, MD, PhD; Sakae Okumura, MD; Yuichi Ishikawa, MD, PhD; Ken Nakagawa, MD; Takeshi Horai, MD; and Makoto Nishio, MD

Background: **Somatic mutations of epidermal growth factor receptor (EGFR) are closely associated with an objective response to *EGFR* tyrosine kinase inhibitors. However, it is difficult to obtain sufficient tumor samples from patients with non-small cell lung cancer (NSCLC), so these diagnoses are often made using cytology procedures alone. The aim of this study was to detect *EGFR* mutations in transbronchial needle aspiration (TBNA) samples using both direct sequencing and a highly sensitive assay (Scorpions Amplified Refractory Mutation System; DxS; Manchester, UK) [ARMS], and to compare the sensitivity of these methods.**

Methods: **We enrolled 94 patients (63 men and 31 women) with NSCLC in this study. Cytologic diagnoses were adenocarcinoma (n = 58), squamous cell carcinoma (n = 24), and other types of NSCLC (n = 12). We extracted DNA from the TBNA samples, and *EGFR* mutations were analyzed using both direct sequencing (exons 19 and 21) and the Scorpions ARMS method (E746 A750del and L858R).**

Results: **Mutations were detected in 31 patients (33%; 14 women and 17 men). Of these, 23 patients had adenocarcinoma, 4 had squamous cell carcinoma, and 4 had other types of NSCLC. Direct sequencing detected 13 mutations (14%) in 13 patients (E746-A750del, n = 6; L858R, n = 7), and the Scorpions ARMS method detected 27 mutations (29%) in 27 patients (E746 A750del, n = 16; L858R, n = 11 patients).**

Conclusions: **Both methods detected *EGFR* mutations in TBNA samples, but Scorpions ARMS is more sensitive than direct sequencing.** ***(CHEST 2007; 131:1628–1634)***

Key words: epidermal growth factor receptor; epidermal growth factor receptor mutation; epidermal growth factor receptor tyrosine kinase inhibitor; Scorpions Amplified Refractory Mutation System; transbronchial needle aspiration

Abbreviations: ARMS = Amplified Refractory Mutation System; Ct = cycle threshold; EGFR = epidermal growth factor receptor; NSCLC = non-small cell lung cancer; PCR = polymerase chain reaction; TBLB = transbronchial lung biopsy; TBNA = transbronchial needle aspiration

Lung cancer is among the most common malignancies worldwide and one of the few types of cancer with an increasing incidence. Advanced non-small cell lung cancer (NSCLC) is treated with a combination of chemotherapy and radiotherapy, but the outcome remains poor. Gefitinib and erlotinib are inhibitors of the tyrosine kinase activity of epi-

*From the Thoracic Center (Drs. Horiike, Ohyanagi, Satoh, Okumura, Nakagawa, Horai, and Nishio) and Department of Pathology (Dr. Ishikawa), Cancer Institute Hospital, Japanese Foundation for Cancer Research; and Shien-Lab (Drs. Kimura and Nishio), National Cancer Center Hospital, Tokyo, Japan.

This work was performed at Cancer Institute Hospital, Japanese Foundation for Cancer Research.

This work was partially supported by funds for the Third Term Comprehensive 10-Year Strategy for Cancer Control and a Grant-in-Aid for Scientific Research.

The authors have no conflicts of interest to disclose.

Manuscript received July 18, 2006; revision accepted January 9, 2007.

Correspondence to: Makoto Nishio, MD, Cancer Institute Hospital, Ariake 3–10-6, Koto-ku, 135-8550, Tokyo, Japan; e-mail: mnishio@jfcr.or.jp

DOI: 10.1378/chest.06-1673

dermal growth factor receptor (EGFR), and have recently been used to treat advanced NSCLC.[1] These agents are dramatically effective in some

For editorial comment see page 1619

patients yet completely ineffective in others. The response rate to gefitinib is high among individuals with an Asian background.[2]

In May and June of 2004, two independent groups reported an association between somatic *EGFR* mutations and a dramatic clinical response to gefitinib, respectively.[3,4] Thereafter, *EGFR* mutations were extensively investigated.[5–17] The mutations consist of small, in-frame deletions or substitutions clustered around the adenosine triphosphate-binding site in exons 18, 19, and 21 of the *EGFR* gene, and approximately 90% of patients with *EGFR* mutations have one of two major mutations. One is a 15-base pair nucleotide in-frame deletion (E746 A750del) in exon 19, and the other is a point mutation involving the replacement of leucine with arginine at codon 858 (L858R) in exon 21.[18] The above studies included genetic analyses of surgical tissues or biopsy specimens. However, to obtain sufficient amounts of tumor samples from inoperable NSCLC patients is often difficult. Some studies[19,20] of patients with advanced NSCLC have found a correlation between clinical manifestations and *EGFR* mutation status obtained from small tumor samples, such as those obtained using standard transbronchial lung biopsy (TBLB). All of the above studies are limited by the fact that the rate of usable samples obtained from enrolled patients is very low. Therefore, a method is required to detect mutant *EGFR*, especially the two major mutations, using samples other than surgical tissues from NSCLC patients. We addressed this problem using a sensitive technique for actual tumor sampling, and a highly sensitive assay for detecting *EGFR* mutations.

Pulmonary lesions are most often clinically diagnosed using flexible bronchoscopy. Common bronchoscopic sampling techniques used for pulmonary lesions are transbronchial needle aspiration (TBNA) and TBLB. One report has indicated that TBNA is superior to TBLB in diagnosing pulmonary lesions: Gasparini et al[21] found that the diagnostic sensitivity of these techniques is 50.0% for TBLB, 70.1% for TBNA, and 76.0% for TBLB and TBNA together. We thus presumed that TBNA is a highly sensitive means of tumor sampling, and that DNA obtained from such specimens might provide useful information about the mutation status of the *EGFR* gene.

We postulated that Scorpions Amplified Refractory Mutation System (ARMS) [DxS; Manchester, UK] technology would enhance the sensitivity of detecting *EGFR* mutations. Scorpion primers are used with a fluorescence-based method that specifically detects polymerase chain reaction (PCR) products.[22] A "scorpion" consists of a specific probe sequence held in a hairpin loop configuration by complementary stem sequences on the 5′ and 3′ ends of the probe. A scorpion can be combined with ARMS to enable the detection of single-base mutations.[22,23] The ARMS method is used for allele discrimination, and additional mismatches have been introduced near the 3′ termini of the primers to enhance specificity. The ARMS method is superior to both direct sequencing and the WAVE method (Transgenomic; Omaha, NE) for detecting *EGFR* mutations.[24] Here, we aimed to detect major *EGFR* mutations in TBNA specimens and to verify the sensitivity of these methods for detecting *EGFR* mutations.

Materials and Methods

Patients

We studied patients with NSCLC diagnosed using specimens obtained by TBLB and/or TBNA. Tumors in saline solution were not collected from enlarged lymph nodes only. After obtaining written informed consent from the patients to participate in all study protocols approved by the Institutional Review Board of the Cancer Institute Hospital, tumor tissues, tumors in saline solution obtained using TBNA, and clinical data were collected. We recorded age at diagnosis, gender, cytologic diagnosis of NSCLC, clinical stage, and smoking status. Cytologic diagnoses were based on the World Health Organization pathology classification. Clinicopathologic staging was determined according to the International Union Against Cancer TNM classification of malignant tumors. Nonsmokers were defined as those who had smoked < 100 cigarettes in their lifetime. We obtained detailed information about smoking history, including age at first cigarette, packs per day, and number of smoking and smoke-free years (after quitting). Patients were categorized as follows: never smoked (< 100 lifetime cigarettes), former smokers (quit ≥ 1 year ago), or current smokers (quit < 1 year ago).

TBNA Sampling

Four experienced operators performed standard flexible bronchoscopy (Olympus P260F; Olympus; Tokyo, Japan) using 21-gauge cytology needles and aspirated for 10 s in the standard fashion.[25] Paired samples consisted of two aspirates that were obtained in immediate succession in an identical manner, with the needle insertion points ideally 1 mm apart. At least four aspirates (two pairs) were obtained from each site. For cytologic analysis, the aspirate was immediately placed onto a glass slide, covered with a second slide, and the slides were drawn apart under continuous gentle pressure. The smear was spray-fixed using ethanol, processed routinely and visualized by Papanicolaou staining. The second aspirate was mixed into 2 mL of saline solution and stored at − 80°C until DNA extraction.

DNA Extraction

Samples obtained by TBNA in saline solution were digested with proteinase K, and then DNA was extracted with phenol-

chloroform and precipitated with ethanol. Precipitated DNA was eluted in 50 μL of sterile, double-distilled water. The concentration and purity of the extracted DNA were determined by spectrophotometry and then the DNA was stored at − 20°C.

PCR Amplification and Direct Sequencing

Genomic PCR was performed in 25-μL volumes using 50 ng of template DNA, 0.75 U of AmpliTaq Gold DNA polymerase (Perkin-Elmer; Roche Molecular Systems; Branchburg, NJ), 2.5 μL of PCR buffer (Perkin-Elmer), 0.8 μmol/L deoxynucleotide triphosphate (Perkin-Elmer), 0.5 μmol/L of each primer, and various concentrations of $MgCl_2$, depending on the polymorphic marker. Exons 19 and 21 were amplified by nested PCR. Primer sequences were obtained as described by Lynch et al.[3] Initial PCR analyses proceeded in a volume of 25 μL as follows: 35 cycles of denaturation at 94°C for 45 s, primer annealing at 58°C for 30 s, and elongation at 72°C for 30 s. A final extension proceeded at 72°C for 10 min. Nested PCR was performed using 20 cycles under the same conditions as the initial PCR. The bands of PCR products were visualized using a 2100 bioanalyzer and the DNA 500 Labchip kit (Agilent Technologies; Palo Alto, CA). Each sample was sequenced in duplicate in both forward and reverse directions using the BigDye Terminator kit (Applied Biosystems; Foster City, CA) and an ABI prism 310 (Applied Biosystems) according to manufacturer instructions. The sequences were then compared with the GenBank-archived human sequence for *EGFR* (accession number AY588246).

Scorpions ARMS for the Detection of E746 A750del and L858R

We used the EGFR Scorpions kit, which combines two technologies, namely ARMS and Scorpions, to detect mutations in real-time PCR reactions. All reactions proceeded in 25-μL volumes using 1 μL of template DNA, 7.5 μL of reaction buffer mix, 0.6 mL of primer mix, and 0.1 mL of Taq polymerase. Real-time PCR was performed using a SmartCycler II (Cepheid; Sunnyvale, CA) under the following conditions: initial denaturation at 95°C for 10 min, 50 cycles of 95°C for 30 s, and 62°C for 60 s with fluorescence reading (set to FAM, which allows optical excitation at 480 nm and measurement at 520 nm) at the end of each cycle. Data were analyzed using Cepheid SmartCycler software (Version 1.2b). The cycle threshold (Ct) was defined as the cycle at the highest peak of the second derivative curve that represented the point of maximum curvature of the growth curve. Both Ct and maximum fluorescence were used for interpretation of the results. Positive results were defined as $Ct \leq 45$ and maximum fluorescence intensity ≥ 30. When only the curve that indicated the wild-type increased, the sample was considered wild-type with respect to *EGFR*. When both wild- and mutant-type curves increased, the sample was considered mutant-type with respect to *EGFR*. These analyses were performed in duplicate for each sample.

Statistical Analysis

The rates of *EGFR* mutation between the two groups were compared using χ^2 or Fisher exact tests. The latter test was applied to five or fewer observations in a group. We used logistic regression models to further explore observed differences and to identify baseline factors that might independently predict an *EGFR* mutation. Probability values of < 0.05 were defined as being statistically significant. All statistical tests were two sided.

RESULTS

Patient Characteristics

Ninety-four patients were enrolled in this study (63 men and 31 women; median age, 66 years) [Table 1]. Among these, 58 patients had adenocarcinoma, 24 patients had squamous cell carcinoma, 5 patients had large cell carcinoma, 2 patients had other classifications of NSCLC, and 5 patients had unclassified NSCLC. Disease in 70 patients was diagnosed from both TBNA and TBLB samples, disease in 23 patients was diagnosed using only TBNA samples, and disease in 1 patient was diagnosed using TBLB samples alone (Table 2). The DNA from TBNA samples in all 93 patients was extracted at a median concentration of 8.7 ng/μL (range, 0.1 to 39.0 ng/μL).

Detection of EGFR Mutations Using Direct Sequencing

We performed direct sequencing in all patients. We could determine *EGFR* mutation status using direct sequencing in samples from 83 patients. We could not evaluate the mutation status of the other 10 patients because we did not obtain sufficient PCR products; bands were undetectable for these 10 patients. In 13 of the 83 patients (15.7%), *EGFR* mutations were detected using direct sequencing. All 13 were heterozygous. E746 A750del was detected in five patients, E746 A752del insA was detected in

Table 1—*Patient Characteristics*

Characteristics	No.	EGFR Mutation, No. (%)
Patients	94	31 (33.0)
Gender		
Male	63	17 (27.0)
Female	31	14 (45.1)
Age, yr		
Mean	67	
Range	26–86	
Stage		
I	44	11 (25.0)
II	3	0 (0)
III	28	13 (46.4)
IV	15	6 (40.0)
Recurrence after surgery	4	1 (25.0)
Cytologic diagnosis		
Adenocarcinoma	58	23 (39.7)
Squamous cell carcinoma	24	4 (16.7)
Large cell carcinoma	5	0 (0)
Other	2	1 (50.0)
Unclassified	5	3 (60.0)
Smoking history		
Current	26	7 (26.9)
Former	34	10 (29.4)
Never	34	14 (41.2)

Table 2—*Diagnostic Yield of Different Bronchoscopic Sampling Techniques

TBLB	TBNA Positive	TBNA Negative
Positive	70 (74.4)	1 (1.1)
Negative	23 (24.5)	

*Data are presented as No. (%).

one patient, and L858R was detected in seven patients. E746 A750 deletion and L858R substitution mutations were frequent (12 of 13 patients with detectable *EGFR* mutations; 92.3%). Figure 1 shows the results of direct sequencing in a patient with E746 A750del (patient 50; Fig 1, *top, A*), and a patient with L858R (patient 70; Fig 1, *bottom, B*). None of the patients had more than one mutation.

Mutation Analysis Using the Scorpions ARMS Method

We performed Scorpions ARMS in all patients. We could analyze *EGFR* mutation status of 91 patients using the *EGFR* Scorpions kit. Because curves corresponding to neither the wild-type nor the mutant-type were detectable in two patients, we could not determine their *EGFR* mutation status. NSCLC was diagnosed in another patient with TBLB alone. Curves corresponded to *EGFR* mutations in 27 patients, indicated the E746 A750del in exon 19 in 16 patients, and indicated L858R in exon 21 in 11 patients (Fig 2).

Comparison of the Two Methods for Detecting the Two Major Mutations

EGFR mutations were detected in 31 patients (Table 3). Both methods together could determine mutation status in 9 patients, whereas either Scorpions ARMS or direct sequencing could do so in 18 patients and 4 patients, respectively. The *EGFR* mutations were more frequently detected by the Scorpions ARMS method than by direct sequencing (Table 4).

EGFR Mutation Status and Clinical Manifestations

The frequency of *EGFR* mutations was higher in patients with adenocarcinomas (23 of 58 patients, 39.7%; vs 8 of 36 patients, 22.2% in nonadenocarcinomas), women (14 of 31 patients, 45.2%; vs 17 of 62 patients, 27.4% in males), and nonsmokers (14 of 34 patients, 41.2%; vs 17 of 59 patients, 28.8% of current or former smokers), although the differences were not statistically significant. The *EGFR* status detected by direct sequencing alone was not statistically correlated with cytologic diagnosis, gender, or response to gefitinib (data not shown).

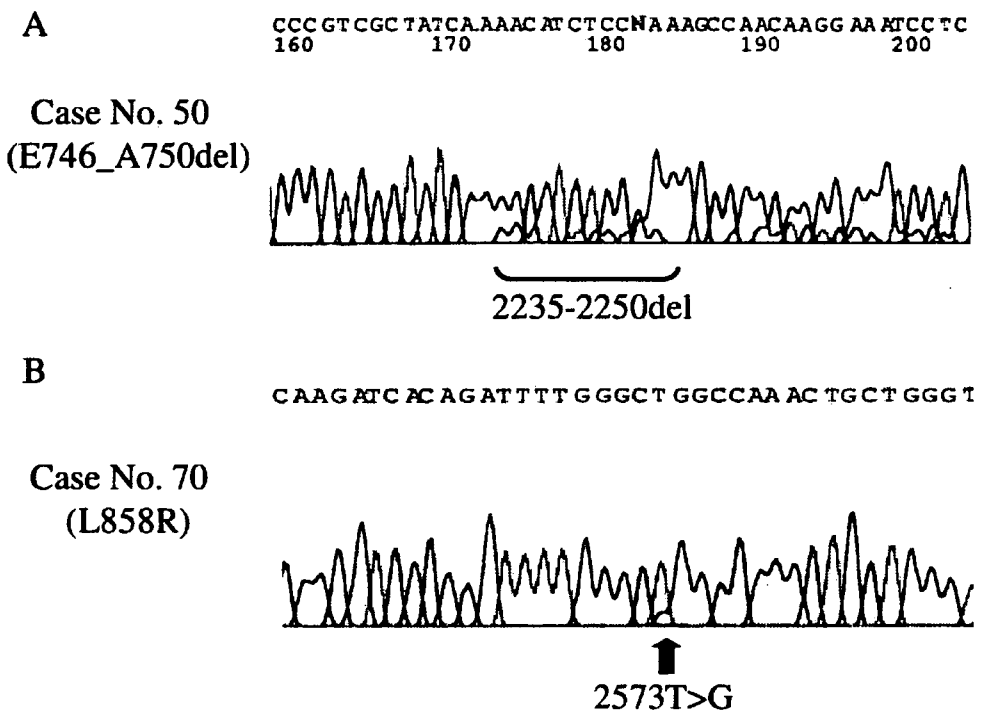

FIGURE 1. Wave figures generated by direct sequencing. *Top, A*: E746 A750 del in exon 19. *Bottom, B*: L858R in exon 21. All mutations were confirmed bidirectionally with forward and reverse sequencing.

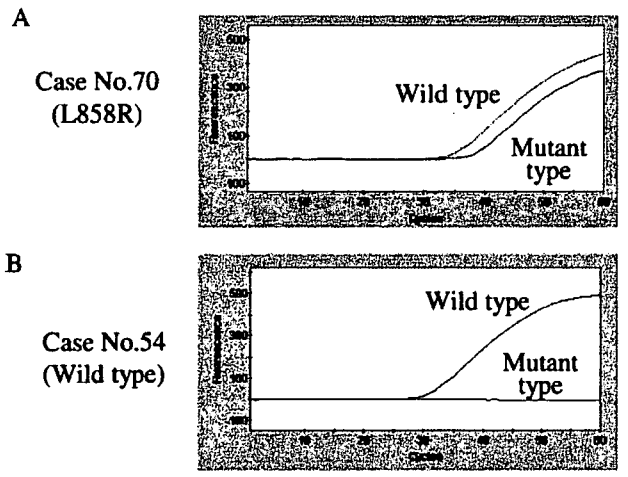

FIGURE 2. Curves for exon 21 using the Scorpions ARMS method. *Top, A*: L858R. *Bottom, B*: wild-type. *Top, A*: Curves for both wild-type and mutant-type have increased, so this sample was considered mutant-type with respect to *EGFR*. *Bottom, B*: Only one curve indicating the presence of wild-type has increased, so the sample was considered wild-type with respect to *EGFR*.

Correlation With Responsiveness to Tyrosine Kinase Inhibitors

Only two patients received gefitinib, one of whom was a 63-year-old woman with a cytologic diagnosis of adenocarcinoma who had never smoked (patient 70). She had partially responded to gefitinib administered from September 2005 to August 2006. Her mutation status according to both direct sequencing and the Scorpions ARMS methods was L858R (Table 3). The other patient was a 69-year-old woman with a cytologic diagnosis of adenocarcinoma who had also never smoked (patient 94). Her condition had stabilized in response to gefitinib that had been administered from August 2005 to October 2005. We determined her mutation status as wild-type in exons 19 and 21.

DISCUSSION

We demonstrated the feasibility of detecting *EGFR* mutations in DNA from TBNA samples from NSCLC patients. Furthermore, we showed that the diagnostic sensitivity of TBNA in our patients was higher than that of TBLB, which agreed with reported findings. The volume of DNA extracted from TBNA samples was measurable by spectrophotometry using our methods and was sufficient to analyze *EGFR* mutation status. Therefore, TBNA samples are apparently suited to such analysis. The mutation rate in this study was lower (33.3%) than that found by other studies of Japanese NSCLC patients.[11,12] However, in line with previous results, we detected *EGFR* mutations at a higher frequency in women, adenocarcinoma patients, and nonsmokers.[6,9] We did not find a relationship between *EGFR* mutation status and response to EGFR tyrosine kinase inhibitors such as gefitinib. Only two patients had already received gefitinib at the time the study was implemented, and the others were to receive gefitinib as a second-line (or later) treatment. The relationship between *EGFR* mutation status and response to gefitinib will be determined in the near future.

The results of this study suggest that the Scorpions ARMS method is more sensitive than direct sequencing for detecting the two major *EGFR* mutations. Direct sequencing is currently the routine method of detecting *EGFR* mutations in tumor samples, and a standard method for detecting *EGFR* mutations in tumor specimens other than surgical tissues has been established. Our results indicated that the *EGFR* Scorpions Kit is superior to direct sequencing for detecting *EGFR* mutations, especially the major deletion mutations in exon 19 and L858R. We previously showed that *EGFR* mutation status in serum DNA detected using the Scorpions ARMS method is a useful predictive marker of the response to gefitinib. That study showed that Scorpions ARMS is more sensitive than direct sequencing for detecting *EGFR* mutations in a mixture of normal and mutant DNA.[26] We inferred from these results that the differences in the determined mutation status for the 18 patients who tested positive using Scorpions ARMS and negative using direct sequencing are due to the density of tumor cells in the sample. However, the reason for the differences in the determined mutation status for those patients who tested negative using Scorpions ARMS and positive using direct sequencing remains obscure. The two methods detected different mutations in the same patient (patient 58), indicating that the primer for the deletion mutation of exon 19 can detect not only E746 A750del but also E746 S752del insA in the Scorpions ARMS method. The differences were frequent in patients with L858R in exon 21 (21.4% of patients with L858R, 5.9% of patients with other mutations). The sensitivity of Scorpions ARMS for detecting L858R was approximately equivalent to that for the detection of E746 A750del in our previous study. Some reports[19,27] have indicated that the presence of *EGFR* gene amplification is more predictive of responses than *EGFR* mutation. However, this does not alter the fact that an *EGFR* mutation is one predictor of response. To detect EGFR gene amplification from cytology samples is complicated by the difficulty of defining fluorescent *in situ* hybridization. Because there were few cancer cells in cytology samples, and these samples did not yield interpretable signals (data not shown).

Table 3—*EGFR Mutation Status and Characteristics of Patients With Mutations

Patient No.	Cytologic Diagnosis	Gender	Age, yr	Smoking History	Mutation Status	
					Direct Sequencing	Scorpions ARMS
50	Ad	Male	63	Former	E746_A750del	E746_A750del
54	Ad	Male	49	Former	E746_A750del	E746_A750del
58	Ad	Male	57	Former	E746_S752del insA	E746_A750del
87	Ad	Female	75	Never	E746_A750del	E746_A750del
91	Ad	Female	69	Never	E746_A750del	E746_A750del
47	Ad	Male	74	Former	E746_A750del	Wild-type
12	NS	Male	86	Former	Wild-type	E746_A750del
22	Ad	Male	67	Current	Wild-type	E746_A750del
28	Ad	Female	56	Current	Wild-type	E746_A750del
40	Ad	Male	52	Current	Wild-type	E746_A750del
43	Sq	Male	70	Former	Wild-type	E746_A750del
44	Ad	Female	72	Never	Wild-type	E746_A750del
49	Ad	Male	73	Former	Wild-type	E746_A750del
67	Ad	Male	76	Former	Wild-type	E746_A750del
77	NS	Male	62	Current	Wild-type	E746_A750del
79	Ad	Female	66	Never	Wild-type	E746_A750del
92	NS	Male	68	Current	Wild-type	E746_A750del
4	Ad	Female	55	Never	L858R	L858R
70	Ad	Female	63	Never	L858R	L858R
82	Ad	Male	50	Current	L858R	L858R
89	Ad	Female	55	Never	L858R	L858R
56	Sq	Male	55	Former	L858R	Wild-type
61	Ad	Female	71	Never	L858R	Wild-type
62	Sq	Female	73	Never	L858R	Wild-type
6	Ot	Male	26	Never	Wild-type	L858R
10	Ad	Female	73	Never	Wild-type	L858R
15	Ad	Female	73	Never	Wild-type	L858R
17	Ad	Male	65	Current	Wild-type	L858R
23	Sq	Male	77	Former	Wild-type	L858R
32	Ad	Female	69	Never	Wild-type	L858R
74	Ad	Female	75	Never	Wild-type	L858R

*Ad = adenocarcinoma; Sq = squamous cell carcinoma; NS = unclassified non-small cell carcinoma; Ot = other classification of non-small cell carcinoma.

Some investigators have tried to improve the sensitivity of detecting *EGFR* mutations. The novel peptide nucleic acid-locked nucleic acid PCR clamp method[28] and the mutant-enriched PCR assay[29] are both rapid and sensitive. Although the minimum detectable mutation volumes were not evaluated in these studies, the sensitivity of these methods seems to be comparable to that of Scorpions ARMS and thus sufficient for clinical use. Since the Scorpions ARMS method is simple and very fast, it might be suitable for mutation screening. However, one limitation of the *EGFR* Scorpions kit is that it can detect only mutations targeted by the designed Scorpions primers. Not all *EGFR* mutations are found at the two targeted sites, as some are clustered around the adenosine triphosphate-binding site in exons 18, 19, and 21.[3–6,9,10] Minor variations of deletional mutations in exon 19, such as E747 P753del insS and L747 T751del, and point mutations other than L858R cannot be detected using Scorpions ARMS. Although approximately 90% of NSCLC-associated *EGFR* mutations comprise the two major EGFR mutations,[18] others might be missed using Scorpions ARMS. Moreover, a secondary mutation, a substitution of methionine for threonine at position 790, leads to gefitinib resistance in NSCLC patients with *EGFR* mutations that are responsive to gefitinib.[30,31] These mutation states may also be critical factors for gefitinib therapy. Scorpions primers need to be designed to detect these mutations, and further study using these primers is required. In conclusion, both direct sequencing and Scorpions ARMS can detect *EGFR* mutations in DNA extracted from

Table 4—*EGFR Mutation Analysis of Different Genetic Assays

Variables	E746-A750del	L858R	Total
Direct sequencing	6 (6.5)	7 (7.5)	13 (14.0)
Scorpions ARMS	16 (17.2)	11 (11.8)	27 (29.0)
Total	17 (18.3)	14 (15.0)	31 (33.3)

*Data are presented as No. (%).

TBNA samples obtained from NSCLC patients, but the latter method is more sensitive.

ACKNOWLEDGMENT: We thank Dr. Stephan Little (DxS, Manchester, UK) for providing the EGFR Scorpions kit and for technical support.

REFERENCES

1 Franklin WA, Veve R, Hirsch FR, et al. Epidermal growth factor receptor family in lung cancer and premalignancy. Semin Oncol 2002; 29:3–14

2 Fukuoka M, Yano S, Giaccone G, et al. Multi-institutional randomized phase II trial of gefitinib for previously treated patients with advanced non-small-cell lung cancer (The IDEAL 1 Trial). J Clin Oncol 2003; 21:2237–2246

3 Lynch TJ, Bell DW, Sordella R, et al. Activating mutations in the epidermal growth factor receptor underlying responsiveness of non-small-cell lung cancer to gefitinib. N Engl J Med 2004; 350:2129–2139

4 Paez JG, Janne PA, Lee JC, et al. EGFR mutations in lung cancer: correlation with clinical response to gefitinib therapy. Science 2004; 304:1497–1500

5 Pao W, Miller V, Zakowski M, et al. EGF receptor gene mutations are common in lung cancers from "never smokers" and are associated with sensitivity of tumors to gefitinib and erlotinib. Proc Natl Acad Sci U S A 2004; 101:13306–13311

6 Kosaka T, Yatabe Y, Endoh H, et al. Mutations of the epidermal growth factor receptor gene in lung cancer: biological and clinical implications. Cancer Res 2004; 64:8919–8923

7 Huang M-J, Lim K-H, Tzen C-Y, et al. EGFR mutations in malignant pleural effusion of non-small cell lung cancer: a case report. Lung Cancer 2005; 49:413–415

8 Marchetti A, Martella C, Felicioni L, et al. EGFR mutations in non-small-cell lung cancer: analysis of a large series of cases and development of a rapid and sensitive method for diagnostic screening with potential implications on pharmacologic treatment. J Clin Oncol 2005; 23:857–865

9 Shigematsu H, Lin L, Takahashi T, et al. Clinical and biological features associated with epidermal growth factor receptor gene mutations in lung cancers. J Natl Cancer Inst 2005; 97:339–346

10 Han SW, Kim TY, Hwang PG, et al. Predictive and prognostic impact of epidermal growth factor receptor mutation in non-small-cell lung cancer patients treated with gefitinib. J Clin Oncol 2005; 23:2493–2501

11 Mitsudomi T, Kosaka T, Endoh H, et al. Mutations of the epidermal growth factor receptor gene predict prolonged survival after gefitinib treatment in patients with non-small-cell lung cancer with postoperative recurrence. J Clin Oncol 2005; 23:2513–2520

12 Takano T, Ohe Y, Sakamoto H, et al. Epidermal growth factor receptor gene mutations and increased copy numbers predict gefitinib sensitivity in patients with recurrent non-small-cell lung cancer. J Clin Oncol 2005; 23:6829–6837

13 Parkin DM, Bray F, Ferlay J, et al. Global cancer statistics, 2002. CA Cancer J Clin 2005; 55:74–108

14 Tomizawa Y, Iijima H, Sunaga N, et al. Clinicopathologic significance of the mutations of the epidermal growth factor receptor gene in patients with non-small cell lung cancer. Clin Cancer Res 2005; 11:6816–6822

15 Tokumo M, Toyooka S, Kiura K, et al. The relationship between epidermal growth factor receptor mutations and clinicopathologic features in non-small cell lung cancers. Clin Cancer Res 2005; 11:1167–1173

16 Sonobe M, Manabe T, Wada H, et al. Mutations in the epidermal growth factor receptor gene are linked to smoking-independent, lung adenocarcinoma. Br J Cancer 2005; 93:355–363

17 Mu XL, Li LY, Zhang XT, et al. Gefitinib-sensitive mutations of the epidermal growth factor receptor tyrosine kinase domain in Chinese patients with non-small cell lung cancer. Clin Cancer Res 2005; 11:4289–4294

18 Pao W, Miller VA. Epidermal growth factor receptor mutations, small-molecule kinase inhibitors, and non-small-cell lung cancer: current knowledge and future directions. J Clin Oncol 2005; 23:2556–2568

19 Bell DW, Lynch TJ, Haserlat SM, et al. Epidermal growth factor receptor mutations and gene amplification in non-small-cell lung cancer: molecular analysis of the IDEAL/INTACT gefitinib trials. J Clin Oncol 2005; 23:8081–8092

20 Tsao MS, Sakurada A, Cutz JC, et al. Erlotinib in lung cancer - molecular and clinical predictors of outcome. N Engl J Med 2005; 353:133–144

21 Gasparini S, Zuccatosta L, Zitti P, et al. Integration of TBNA and TCNA in the diagnosis of peripheral lung nodules: influence on staging. Ann Ital Chir 1999; 70:851–855

22 Whitcombe D, Theaker J, Guy SP, et al. Detection of PCR products using self-probing amplicons and fluorescence. Nat Biotechnol 1999; 17:804–807

23 Newton CR, Graham A, Heptinstall LE, et al. Analysis of any point mutation in DNA: the amplification refractory mutation system (ARMS). Nucleic Acids Res 1989; 17:2503–2516

24 Wookey A, Ellison G, Donald E, et al. Comparison of methods for the detection of mutations in the epidermal growth factor receptor gene. Presented at the 96th Annual Meeting of the American Association for Cancer Research, April 16–20, 2005, Anaheim, CA; abstract 5287

25 Dasgupta A, Jain P, Minai OA, et al. Utility of transbronchial needle aspiration in the diagnosis of endobronchial lesions. Chest 1999; 115:1237–1241

26 Kimura H, Kasahara K, Kawaishi M, et al. Detection of epidermal growth factor receptor mutations in serum as a predictor of the response to gefitinib in patients with non-small-cell lung cancer. Clin Cancer Res 2006; 12:3915–3921

27 Hirsch FR, Varella-Garcia M, McCoy J, et al. Increased epidermal growth factor receptor gene copy number detected by fluorescence *in situ* hybridization associates with increased sensitivity to gefitinib in patients with bronchioloalveolar carcinoma subtypes: a Southwest Oncology Group study. J Clin Oncol 2005; 23:6838–6845

28 Nagai Y, Miyazawa H, Huqun, et al. Genetic heterogeneity of the epidermal growth factor receptor in non-small cell lung cancer cell lines revealed by a rapid and sensitive detection system: the peptide nucleic acid-locked nucleic acid PCR clamp. Cancer Res 2005; 65:7276–7282

29 Asano H, Toyooka S, Tokumo M, et al. Detection of EGFR gene mutation in lung cancer by mutant-enriched polymerase chain reaction assay. Clin Cancer Res 2006; 12:43–48

30 Kobayashi S, Boggon TJ, Dayaram T, et al. EGFR mutation and resistance of non-small-cell lung cancer to gefitinib. N Engl J Med 2005; 352:786–792

31 Kwak EL, Sordella R, Bell DW, et al. Irreversible inhibitors of the EGF receptor may circumvent acquired resistance to gefitinib. Proc Natl Acad Sci U S A 2005; 102:7665–7670

Oncogene (2007) 26, 4749–4760

www.nature.com/onc

ORIGINAL ARTICLE

Clock and ATF4 transcription system regulates drug resistance in human cancer cell lines

T Igarashi[1,2], H Izumi[1], T Uchiumi[1], K Nishio[3], T Arao[3], M Tanabe[1], H Uramoto[4], K Sugio[4], K Yasumoto[4], Y Sasaguri[5], KY Wang[5], Y Otsuji[2] and K Kohno[1]

[1]Department of Molecular Biology, School of Medicine, University of Occupational and Environmental Health, Kitakyushu, Japan; [2]Department of Internal Medicine II, School of Medicine, University of Occupational and Environmental Health, Kitakyushu, Japan; [3]Department of Genome Biology, School of Medicine, Kinki University, Osaka, Japan; [4]Department of Surgery II, School of Medicine, University of Occupational and Environmental Health, Kitakyushu, Japan and [5]Department of Pathology II, School of Medicine, University of Occupational and Environmental Health, Kitakyushu, Japan

The mechanisms underlying cellular drug resistance have been extensively studied, but little is known about its regulation. We have previously reported that activating transcription factor 4 (ATF4) is upregulated in cisplatin-resistant cells and plays a role in cisplatin resistance. Here, we find out a novel relationship between the circadian transcription factor Clock and drug resistance. Clock drives the periodical expression of many genes that regulate hormone release, cell division, sleep-awake cycle and tumor growth. We demonstrate that *ATF4* is a direct target of Clock, and that Clock is overexpressed in cisplatin-resistant cells. Furthermore, Clock expression significantly correlates with cisplatin sensitivity, and that the downregulation of either Clock or ATF4 confers sensitivity of A549 cells to cisplatin and etoposide. Notably, ATF4-overexpressing cells show multidrug resistance and marked elevation of intracellular glutathione. The microarray study reveals that genes for glutathione metabolism are generally downregulated by the knockdown of ATF4 expression. These results suggest that the Clock and ATF4 transcription system might play an important role in multidrug resistance through glutathione-dependent redox system, and also indicate that physiological potentials of Clock-controlled redox system might be important to better understand the oxidative stress-associated disorders including cancer and systemic chronotherapy.
Oncogene (2007) **26,** 4749–4760; doi:10.1038/sj.onc.1210289; published online 12 February 2007

Keywords: Clock; ATF4; multidrug resistance; glutathione; chronotherapy

Correspondence: Professor K Kohno, Department of Molecular Biology, School of Medicine, University of Occupational and Environmental Health, 1-1 Iseigaoka Yahatanishi-ku, Kitakyushu, Fukuoka, 807-8555, Japan.
E-mail: k-kohno@med.uoeh-u.ac.jp
Received 2 November 2006; revised 14 December 2006; accepted 20 December 2006; published online 12 February 2007

Introduction

Cisplatin is a potent anticancer agent that is used in the treatment of various solid tumors, but the development of resistance is a major obstacle in a clinical setting (Wang and Lippard, 2005). Several mechanisms are involved in the acquisition of cisplatin resistance, including decreased drug accumulations (Komatsu *et al.*, 2000; Nakayama *et al.*, 2002), increased levels of cellular glutathione (Lai *et al.*, 1989; Tew, 1994), and increased DNA-repair activity (Chaney and Sancar, 1996; Husain *et al.*, 1998). We have been interested in the transcription factors activated in response to cisplatin, which might play a crucial role in cisplatin resistance (Kohno *et al.*, 2005; Torigoe *et al.*, 2005). We believe that the transcription factors of genes involved in cisplatin resistance are often overexpressed or activated in cisplatin-resistant cells.

Activating transcription factor 4 (ATF4) is a member of the cyclic adenosine monophosphate responsive element-binding (CREB) protein family, and is involved in multiple intracellular stress pathways (Rutkowski and Kaufman, 2003). ATF4 is ubiquitously expressed in human cancer cells, and is essential for normal cellular proliferation (Fawcett *et al.*, 1999), especially the high-level proliferation required during fetal liver hematopoiesis (Masuoka and Townes, 2002). ATF4-null cells also show impaired glutathione biosynthesis (Harding *et al.*, 2003). We have shown previously that ATF4 is upregulated in cisplatin-resistant cell lines and is involved in cisplatin resistance (Tanabe *et al.*, 2003).

We herein investigate the molecular regulation of *ATF4* gene expression and drug resistance. Interestingly, a database search revealed an E-box in the core promoter region of *ATF4*, and we show that the essential circadian regulator Clock binds to this E-box and is overexpressed in cisplatin-resistant cells. It has been reported previously that Clock/BMAL1 heterodimers activate transcription from E-box elements (Gekakis *et al.*, 1998); therefore, *ATF4* is thought to be regulated by circadian transcription factors. Down-regulation of either Clock or ATF4 using small interfering RNAs (siRNAs) was shown to confer cell

sensitivity to anticancer agents. Furthermore, ATF4-overexpressing cells showed multidrug resistance and marked elevation of intracellular glutathione. Knock-down of ATF4 expression lead to downregulation of glutathione metabolism. Our findings indicate an important contribution of both Clock and ATF4 to chemosensitivity.

Results

Overexpression of Clock in cisplatin-resistant cells

We have shown previously that the transcription factor ATF4 is overexpressed in cisplatin-resistant cell lines (Tanabe *et al.*, 2003). As an E-box is located in the core promoter region of *ATF4*, we examined the expression levels of the E-box-binding proteins c-Myc, upstream stimulatory factor 1 (USF1), and Clock. Western blotting analysis revealed that the Clock protein was overexpressed in cisplatin-resistant cell lines (Figure 1a). No significant alteration of c-Myc and USF1 expression was observed between parental and cisplatin-resistant cells. As the Clock/BMAL1 complex regulates the expression of circadian genes (Gekakis *et al.*, 1998), we analysed the BMAL1 expression. However, the BMAL1 expression was not upregulated in cisplatin-resistant cells (data not shown). Northern blotting analysis revealed that Clock messenger RNA (mRNA) was also overexpressed in cisplatin-resistant cells (Figure 1b), suggesting that Clock might be involved in the transcriptional regulation of *ATF4* by binding to its promoter E-box.

ATF4 is a direct target of Clock

To test whether the *ATF4* promoter is a direct target of Clock, we carried out chromatin immunoprecipitation (ChIP) assays using specific primer pairs for the *ATF4* promoter region and an anti-Clock antibody. As shown in Figure 1c, this analysis revealed that Clock bound specifically to the E-box region of the *ATF4* promoter. A luciferase reporter gene assay showed that both Clock and BMAL1 co-transfection transactivated the *ATF4* promoter, and that this transactivation was dependent on an intact E-box, as reporter gene expression was reduced following transfection of a mutated E-box (Figure 1d). We also verified the relationship between ATF4 expression and Clock using siRNAs. Inactivation of Clock by siRNA was shown to suppress the promoter activity of *ATF4* gene (Figure 1e) as well as cellular expression level of ATF4 in PC3 cells (Figure 1f).

Cellular expression of Clock correlates with cisplatin sensitivity

To explore whether Clock overexpression is involved in cisplatin resistance, we examined the correlation between Clock expression and cisplatin sensitivity in 11 lung cancer cell lines (Figure 2a). Clock expression significantly correlated with cisplatin sensitivity (Figure 2b) and with ATF4 expression (Figure 2c) in these cell lines, but c-myc expression did not (data not shown). To confirm these findings by an alternative approach, we used the siRNA strategy. Downregulation of the cellular expression of the Clock protein conferred cisplatin and etoposide, but not 5-fluorouracil (5-FU), sensitivity to A549 cells (Figure 2d). Similar results were also obtained when ATF4 expression was downregulated. Clock expression did not correlate with the cellular sensitivity of etoposide, doxorubicin and vincristine at all (data not shown). We next investigated whether downregulation of ATF4 expression overcomes cisplatin resistance in cisplatin-resistant cell line P/CDP6. As shown in Figure 2e, downregulation of ATF4 expression partially overcomes cisplatin resistance, because the IC_{50} value of cisplatin in PC3 cells is about 0.7 μM (data not shown).

Multidrug resistance in ATF4-overexpressing cell lines

In addition to our two previously established ATF4-overexpressing cell lines (Tanabe *et al.*, 2003), we derived two new cell lines that overexpressed ATF4 (A549/ATF4-5 and A549/ATF4-6) at levels 10–20-fold higher than vector-alone transfectants (A549/pcDNA-1 and A549/pcDNA-2) (Figure 4). The ATF4-overexpressing cell lines showed increased resistance to cisplatin, doxorubicin, etoposide, SN-38, and vincristine, but not to 5-FU (Table 1). To our knowledge, this is the first transcription factor that can induce multidrug-resistant phenotypes.

Intracellular glutathione level and drug resistance-related gene expression in ATF4-overexpressing cells

It has been reported that $ATF4^{-/-}$ cells demonstrate impaired glutathione biosynthesis (Harding *et al.*, 2003), whereas an increased level of glutathione has been shown to be involved in drug resistance (Lai *et al.*, 1989; Tew, 1994). Therefore, intracellular glutathione levels were evaluated in ATF4-overexpressing cell lines, and were found to be approximately 12.7-fold higher than in control cells (Figure 3a). This increase was abolished when cells were treated with the γ-glutamylcysteine synthetase inhibitor: buthionine-sulfoximine (BSO) (10 μM). To examine whether Clock and ATF4 are involved in glutathione biosynthesis, A549 cells were transfected with Clock-directed, ATF4-directed, or control siRNA oligomers. Downregulation of both Clock and ATF4 was found to reproducibly suppress intracellular glutathione levels to 75–80% of the control levels (Figure 3b).

It has been shown that resistant cells against cisplatin often upregulate both glutamate-cysteine ligase catalytic subunit (GCLC) and glutathione S-transferase π (GSTπ) (Saburi *et al.*, 1989; Yao *et al.*, 1995). On the other hand, the resistant cells against topoisomerase-targeted drugs often downregulate DNA topoisomerase (Takano *et al.*, 1992). We, therefore, examined drug resistance-related gene expressions in ATF4-overexpressing cells (Figure 4). Although ATF4-overexpressing cells were resistant to etoposide and SN-38, the expressions of DNA topoisomerase I and IIα were not downregulated. As we expected, the expressions of

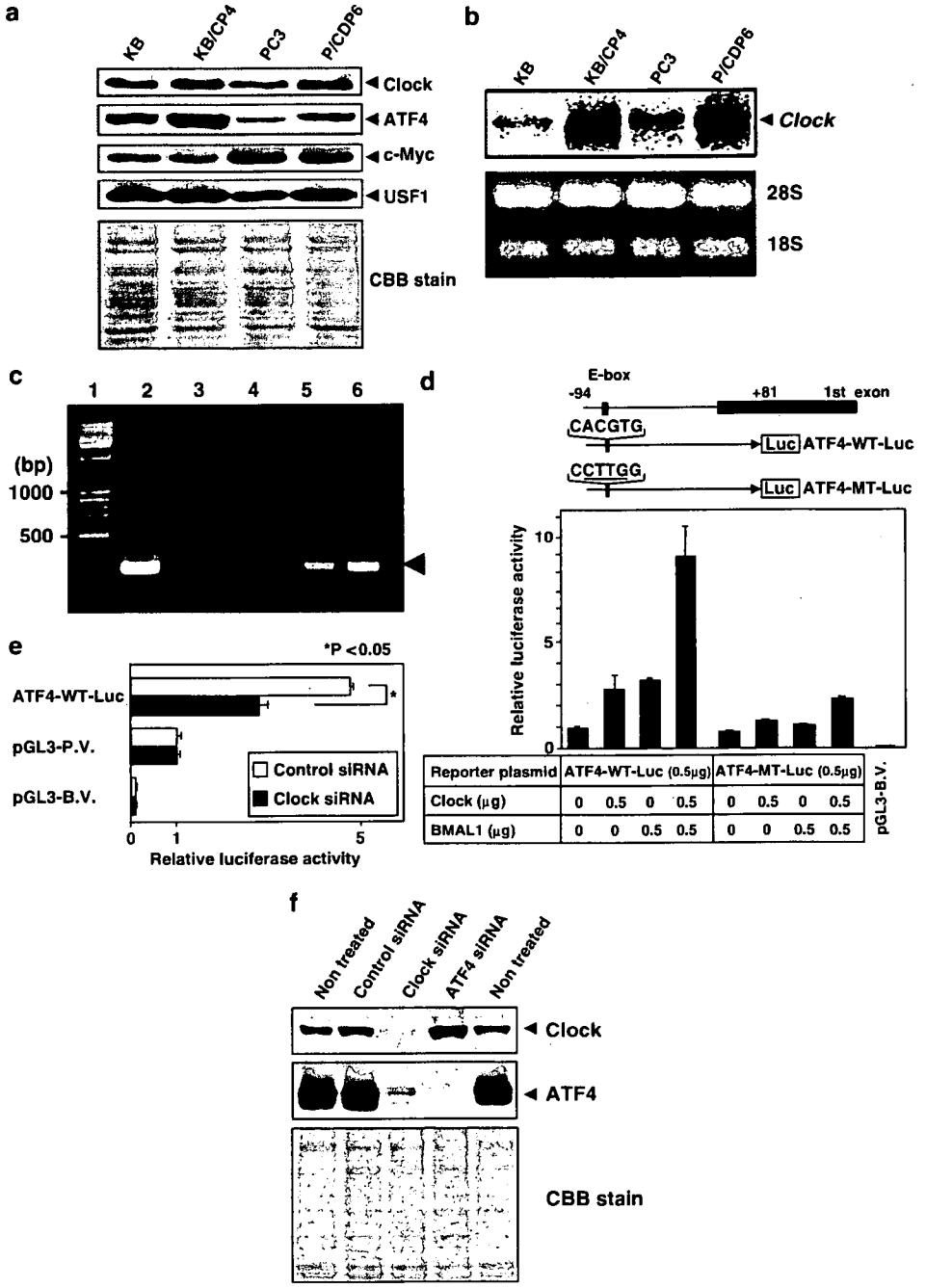

Figure 1 Clock regulates *ATF4* gene expression through binding to the E-box located in the promoter region. (**a**) Whole-cell extracts (75 μg for Clock, and 50 μg for c-Myc and USF1) and nuclear extracts (100 μg for ATF4) were subjected to SDS–PAGE, and Western blotting analysis was performed with the indicated antibodies. Gel staining with Coomassie Brilliant Blue (CBB) is also shown. (**b**) Total RNA (20 μg) prepared from the indicated cells was separated on a 1% formaldehyde-agarose gel and transferred to a Hybond N$^-$ membrane. Northern blotting analysis was performed with a Clock cDNA probe. Gel staining with ethidium bromide is also shown. (**c**) A ChIP assay of the PC3 cells was performed with antibodies against Clock or goat IgG. Immunoprecipitated DNAs (anti-goat IgG in lanes 3 and 4, and anti-Clock IgG in lanes 5 and 6) were amplified by PCR using specific primer pairs for the *ATF4* promoter region. The templates used for PCR were as follows: 1 μl (lane 2) of genomic DNA from cell lysate, and 1 μl (lanes 3 and 5) and 3 μl (lanes 4 and 6) of immunoprecipitated DNAs. Lane 1 contains a DNA size marker. The arrowhead indicates amplified partial *ATF4* promoters (278 bp). (**d**) Indicated amounts of Clock and/or BMAL1 expression plasmids were transiently co-transfected with ATF4-WT-Luc or ATF4-MT-Luc into MCF7 cells. The schematic representation of ATF4-WT-Luc and ATF4-MT-Luc is shown above. pGL3-B.V. indicates pGL3 basic vector. The results are normalized to β-galactosidase activity and are representative of at least three independent experiments. Bars = $\pm$s.d. (**e**) MCF7 cells were transfected with 50 nM control or Clock siRNAs. The following day, they were transfected with the indicated reporter plasmids. The results were normalized to β-galactosidase activity and pGL3 promoter vector (Promega). All values are the mean of at least three independent experiments. pGL3-PV and pGL3-BV indicate pGL3 promoter vector and pGL3 basic vector, respectively. Bars = $\pm$s.d. (**f**) Indicated siRNAs were transfected into PC3 cells. Whole-cell extracts (75 μg) for Clock and nuclear extracts (100 μg) for ATF4 were subjected to SDS–PAGE, and Western blotting analysis was performed.

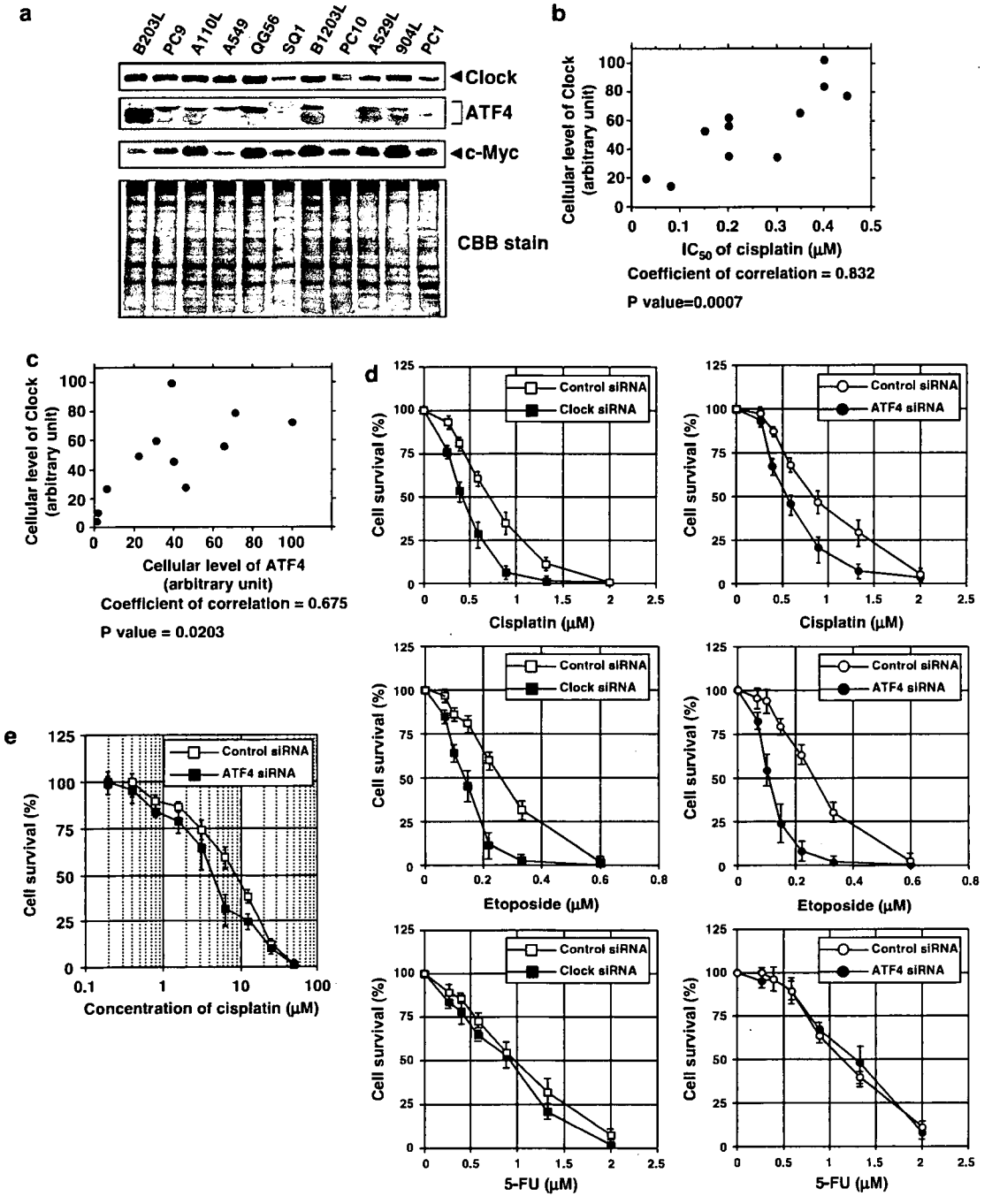

Figure 2 Clock expression correlates with cisplatin resistance and ATF4 expression. (**a**) Western blotting analysis was performed with 100 μg nuclear extracts for ATF4 expression and 75 μg whole-cell extracts for Clock and c-Myc expressions in 11 human lung cancer cell lines. Gel staining with CBB is also shown. (**b**) and (**c**) Expression levels of Clock and ATF4 (whole band) were determined by NIH imaging using Figure 2a, and were normalized by each CBB stain. The maximum expression levels of Clock or ATF4 were set to 100, and the IC_{50} of each cell line was calculated from the concentration–response curves for cisplatin. (**d**) Downregulation of either Clock or ATF4 confers sensitivity of A549 cells to cisplatin and etoposide. Cells were transfected with the indicated siRNAs, and exposed to various concentrations of cisplatin, etoposide, and 5-FU for 7 days. The colony number in the absence of drugs corresponded to 100%. All values are the mean of at least three independent experiments. Bars = $\pm$s.d. (**e**) P/CDP6 cells were transfected with 50 nM control or Clock siRNAs. The following day, various concentrations of cisplatin were treated. After 72 h, cell survival was analysed with a WST-8 assay. Cell survival in the absence of cisplatin corresponded to 100%. All values are the mean of at least three independent experiments. Bars = $\pm$s.d.

GCLC and GSTπ were upregulated in ATF4-overexpressing cells. Drug resistance is also modulated by the expression of both anti-apoptotic and apoptotic molecules. We then examined the expression of several molecules involved in apoptosis such as Bcl-2, Bcl-X_L, Bax and BAK. However, we could not detect the significant alteration between drug-resistant cells and ATF4-overexpressing cells (data not shown). To explore

Table 1 Drug sensitivity (half-maximal inhibitory concentration [IC_{50}]) and relative resistance of ATF4-overexpressing cell lines

	Cell line		
Drug	*A549/pcDNA3*[a]	*A549/ATF4*[b]	*Relative resistance*[c]
5-FU (μM)	1.38 (±0.04)	1.35 (±0.21)	1.0
Cisplatin (μM)	0.67 (±0.04)	2.11 (±0.02)	3.1
Doxorubicin (μM)	0.03 (±0.01)	0.14 (±0.04)	3.6
Etoposide (μM)	0.39 (±0.01)	2.02 (±0.64)	5.2
SN-38 (nM)	5.25 (±1.06)	19.0 (±1.41)	3.6
Vincristine (nM)	2.75 (±0.78)	6.10 (±1.56)	2.2

[a]Control cell lines A549/pcDNA3-1 and A549/pcDNA3-2. [b]ATF4-overexpressing cell lines A549/ATF4-5 and A549/ATF4-6. [c]IC50 ratio of ATF4-overexpressing cell lines to control cell lines. The cell viability after drug exposure was analysed with a WST assay. In the absence of drugs, the viability was 100%. The IC_{50} of each cell line was calculated from the concentration–response curves. All values indicate the mean±standard deviation (s.d.). 5-FU, 5-fluorouracil; SN-38, 7-ethyl-10-hydroxycamptothecin.

a potential role for glutathione, we tested BSO for its ability to reverse drug resistance in ATF4-overexpressing cells, and found that cellular sensitivity of cisplatin and etoposide was almost completely reversed by addition of BSO (Figure 5a and b). We also examined the expression of drug resistance-related genes after BSO treatment. However, no significant alteration of gene expression was observed (data not shown).

Microarray analysis of ATF4-regulated genes

Because the available information regarding the transcriptional regulation by ATF4 was limited, we used microarray technology to enable the simultaneous analysis of large numbers of genes. To confirm further transcriptional changes by the ATF4 siRNA, oligonucleotide microarray study was carried out in A549 cells treated with or without ATF4 siRNA (0.3 nM of ATF4 siRNA downregulated the cellular expression of ATF4 to 50%). Data analysis identified 121 genes, which were downregulated more than 2.5-fold and only eight genes which were upregulated (Supplementary Information). Among downregulated genes, only glutathione peroxidase 2 (GPX2) gene was identified in relation to glutathione metabolism. Then, we analysed the subset of genes for glutathione metabolism. As shown in Figure 6a, the genes for glutathione metabolism were generally downregulated by ATF4 knockdown including GCLC, glutamate-cysteine ligase modifier subunit (GCLM), γ-glutamyltransferase 1 (GGT1), γ-glutamyltransferase 2 (GGT2), glutamic pyruvate transaminase 2 (GPT2), GPX2, glutathione S-transferase M4 (GSTM4) and microsomal glutathione S-transferase 2 (MGST2). The ATF4-binding site was found in the proximal promoter region of these eight genes (data not shown). It was reported that GCLC was a key enzyme to determine the cellular glutathione levels and often involved in drug resistance (Tipnis *et al.*, 1999). To evaluate the microarray study, we carried out Western blotting analysis and revealed that the GCLC expression was downregulated by the ATF4 siRNA (Figure 6b). As

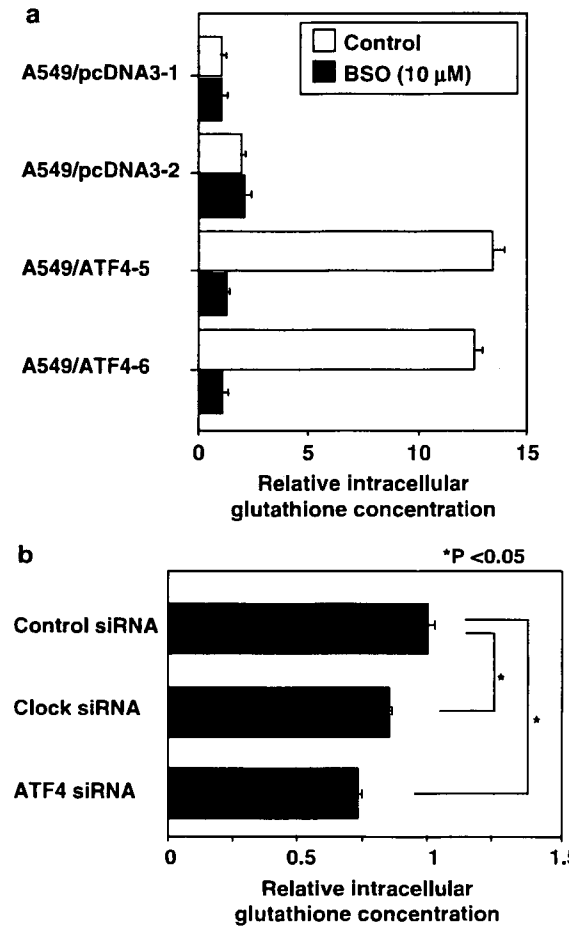

Figure 3 Intracellular glutathione levels are evaluated in ATF4-overexpressing cells and downregulated by Clock or ATF4 siRNAs. (**a**) Intracellular glutathione levels of ATF4-overexpressing cell lines (A549/ATF4-5, 6) and control cell lines (A549/pcDNA3-1, 2) with or without 10 μM BSO treatment for 72 h were measured. Each glutathione concentration indicates a relative level to A549/pcDNA3-1. (**b**) A549 cells were transfected with Clock or ATF4 siRNAs, and intracellular glutathione levels were measured. Each glutathione concentration indicates a relative level to control siRNA. All values are the mean of at least three independent experiments. Bars = ±s.d.

shown in Figure 6c, the expressions of GCLC and GSTπ were significantly upregulated in cisplatin-resistant cells. These data were comparable with our microarray analysis. However, the GCLC expression was not downregulated by the Clock siRNA (data not shown).

The expression of the ATP-binding cassette transporter family

As shown in Table 1, the ATF4-overexpressing cell lines showed multidrug-resistant phenotypes. It has been reported that intracellular glutathione could support the drug efflux by ATP-binding cassette (ABC) transporters (Renes *et al.*, 2000). Thus, we next examined the expression of major ABC transporters such as multidrug resistance protein 1 (MRP1/*ABCC1*), multidrug resistance protein 2 (MRP2/*ABCC2*), breast cancer-resistance protein (BCRP/*ABCG2*) and